Appendix B

Differential FT-LDOS-vs.-energy in $YB_2Cu_3O_{7-\delta}$

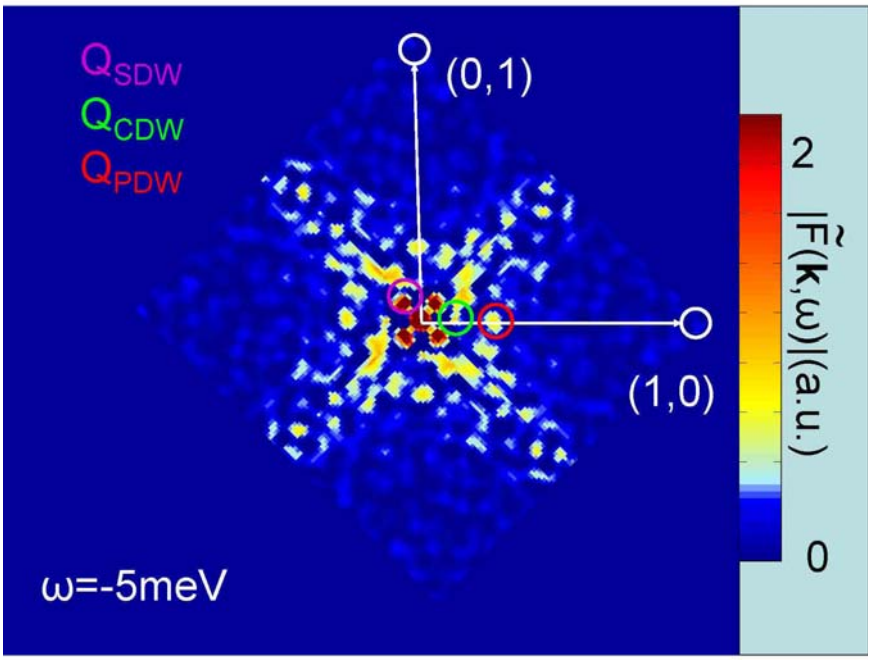

Figure B.1: $\tilde{F}(\mathbf{k},\omega$=-5meV,H=5T)

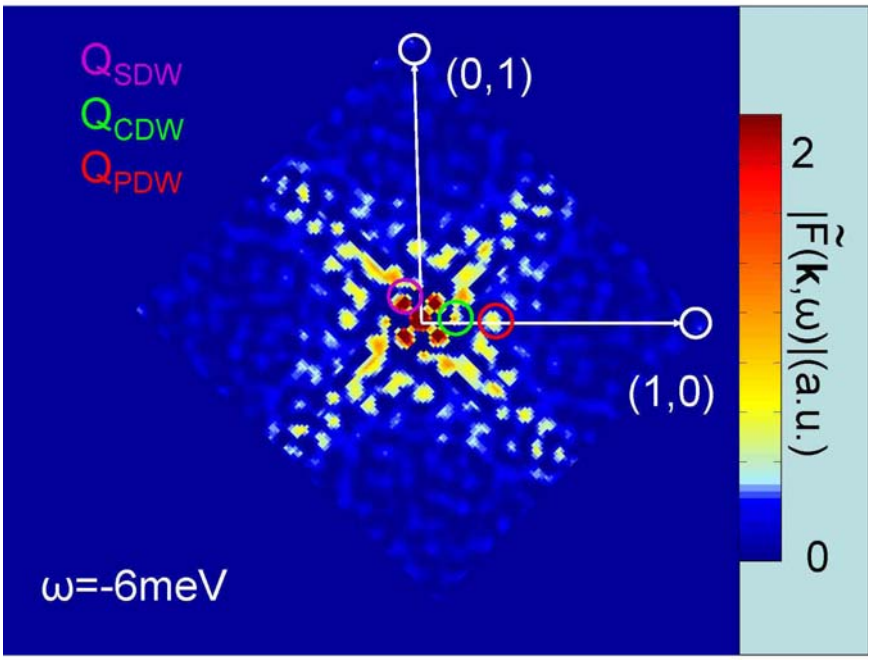

Figure B.2: $\tilde{F}(\mathbf{k},\omega$=-6meV,H=5T)

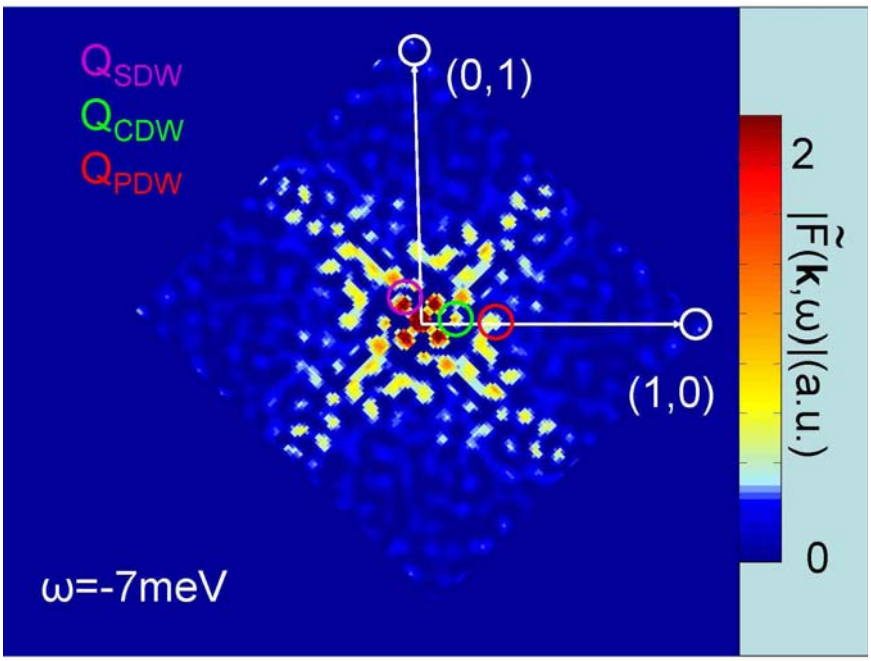

Figure B.3: $\tilde{F}(\mathbf{k},\omega$=-7meV,H=5T)

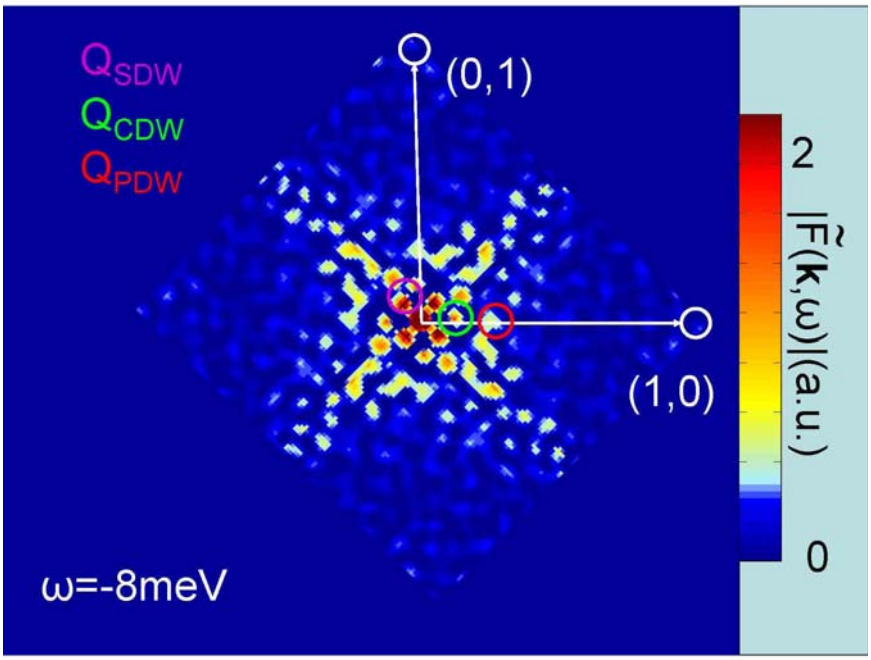

Figure B.4: $\tilde{F}(\mathbf{k},\omega$=-8meV,H=5T)

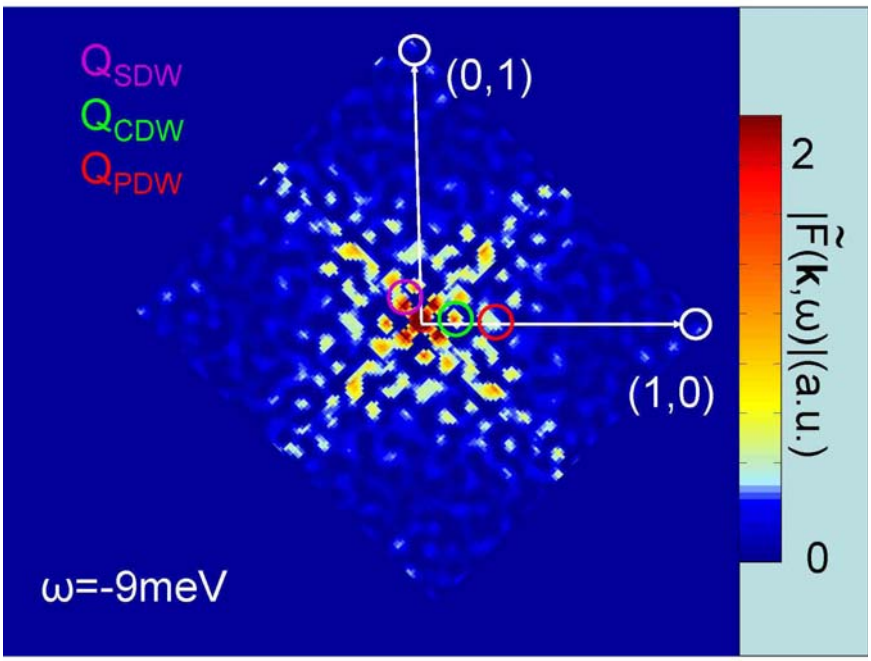

Figure B.5: $\tilde{F}(\mathbf{k},\omega$=-9meV,H=5T)

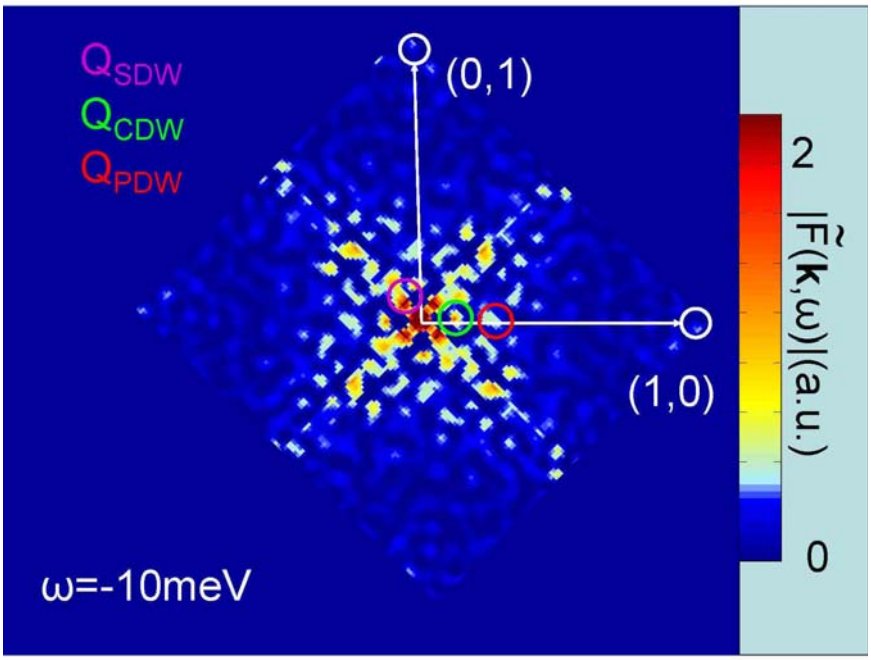

Figure B.6: $\tilde{F}(\mathbf{k},\omega$=-10meV,H=5T)

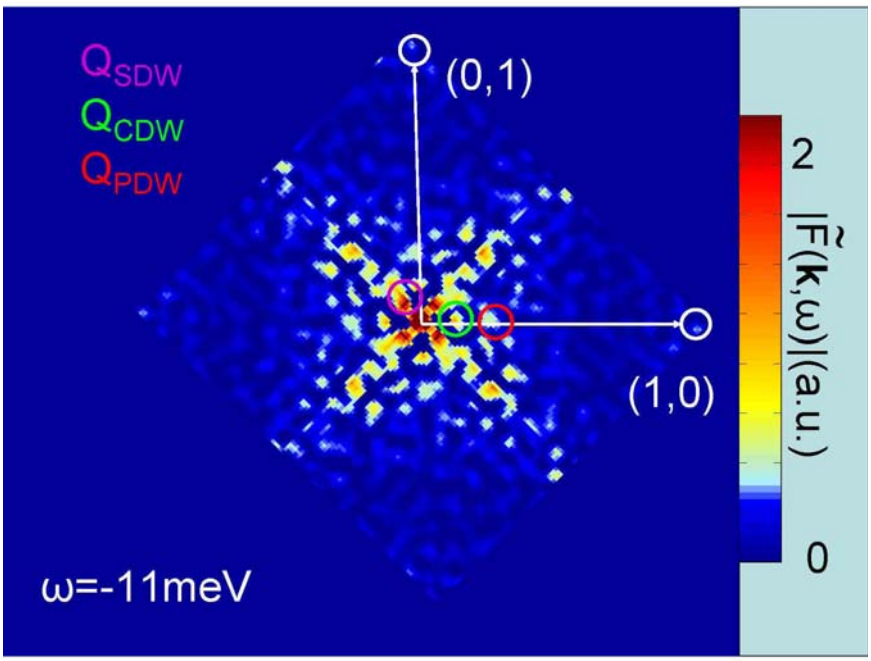

Figure B.7: $\tilde{F}(\mathbf{k},\omega$=-11meV,H=5T)

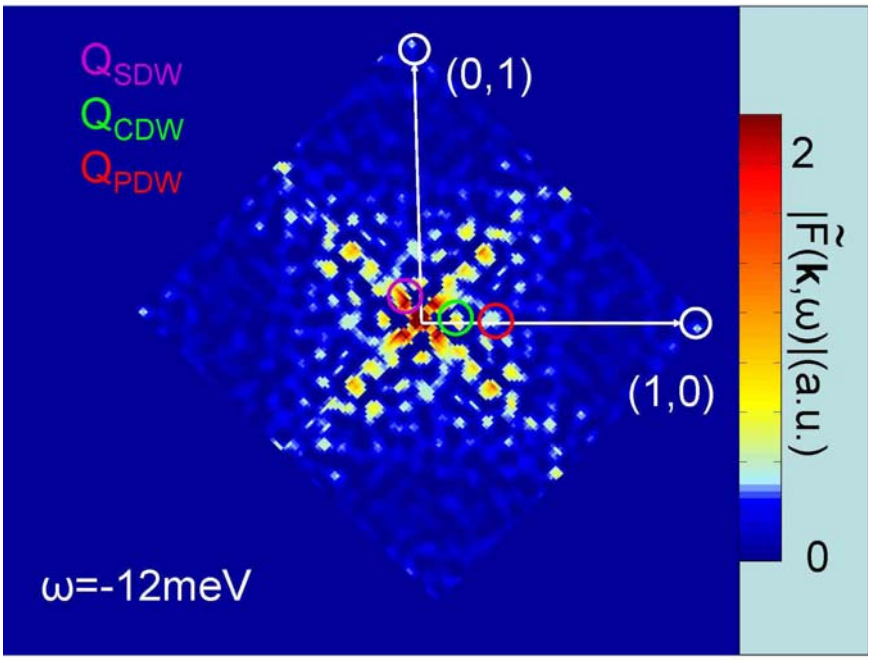

Figure B.8: $\tilde{F}(\mathbf{k},\omega$=-12meV,H=5T)

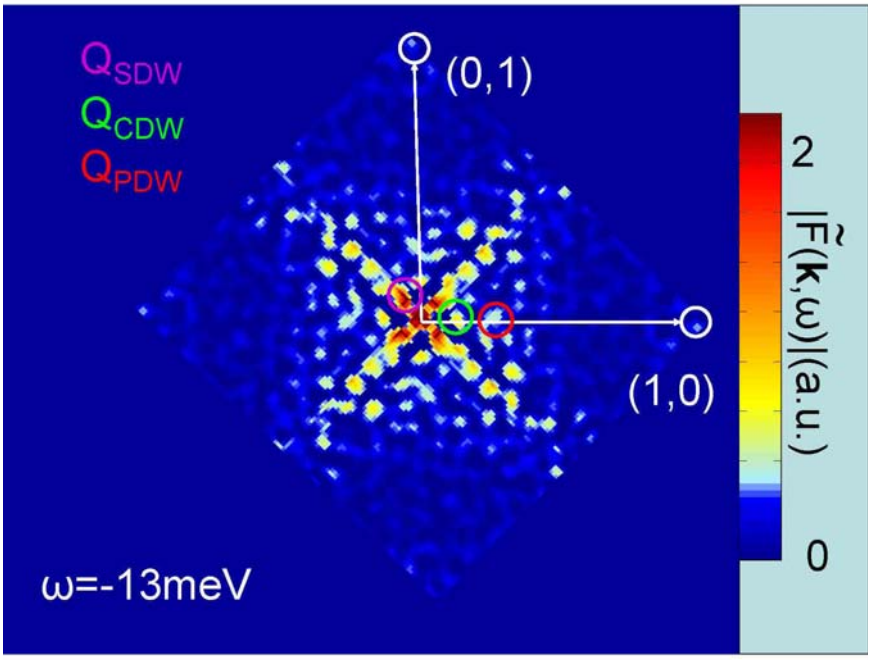

Figure B.9: $\tilde{F}(\mathbf{k},\omega$=-13meV,H=5T)

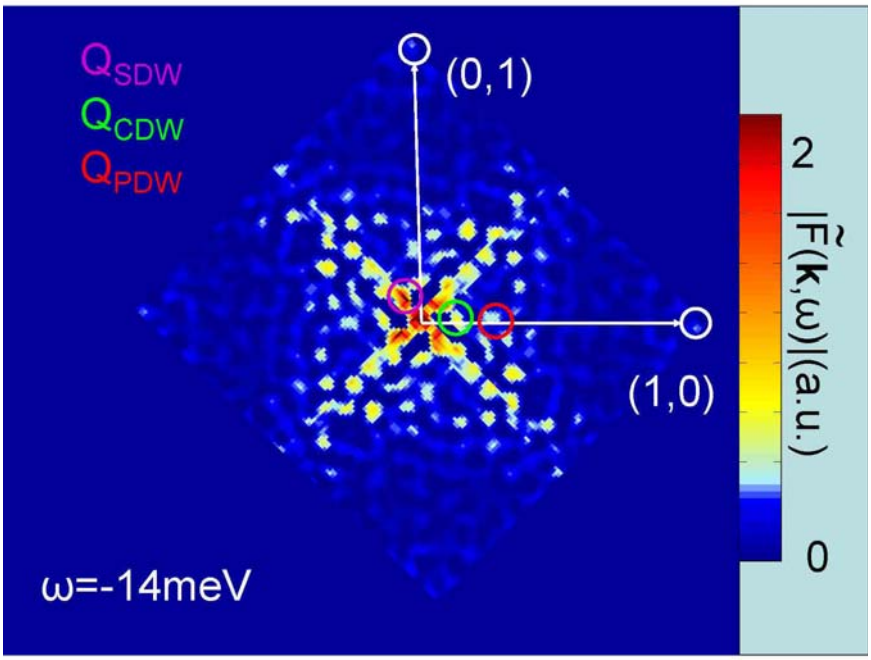

Figure B.10: $\tilde{F}(\mathbf{k},\omega$=-14meV,H=5T)

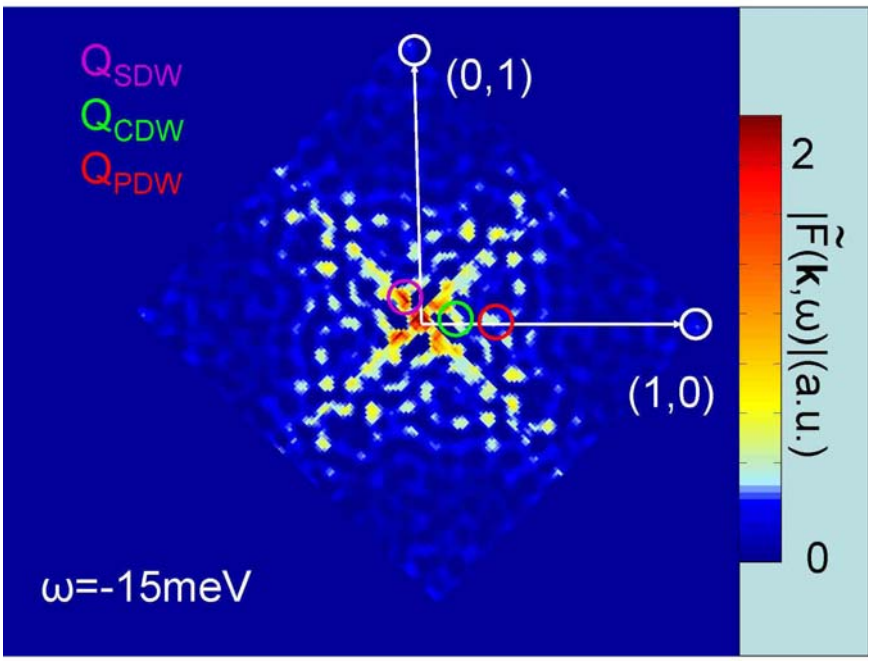

Figure B.11: $\tilde{F}(\mathbf{k},\omega$=-15meV,H=5T)

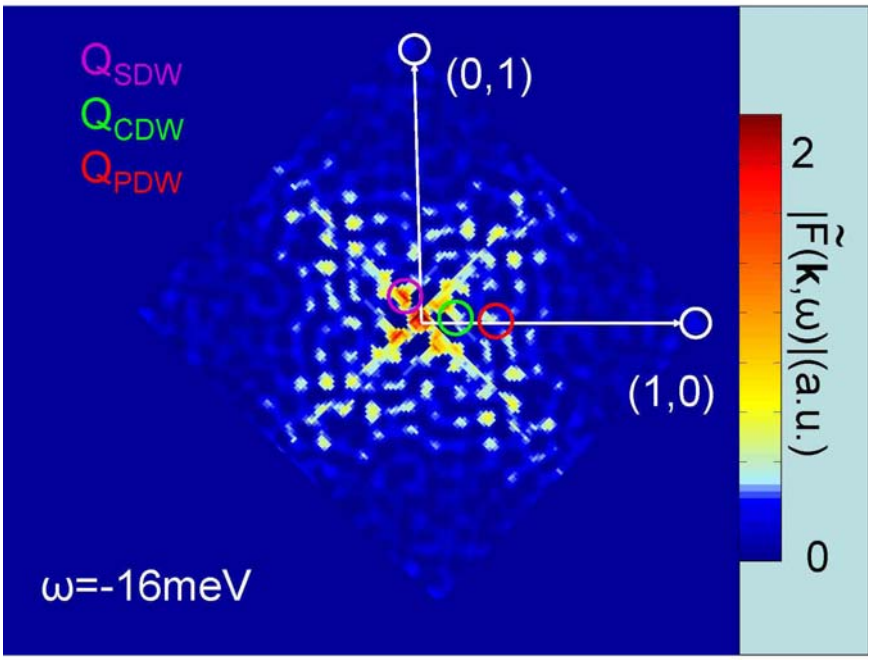

Figure B.12: $\tilde{F}$(**k**,ω=-16meV,H=5T)

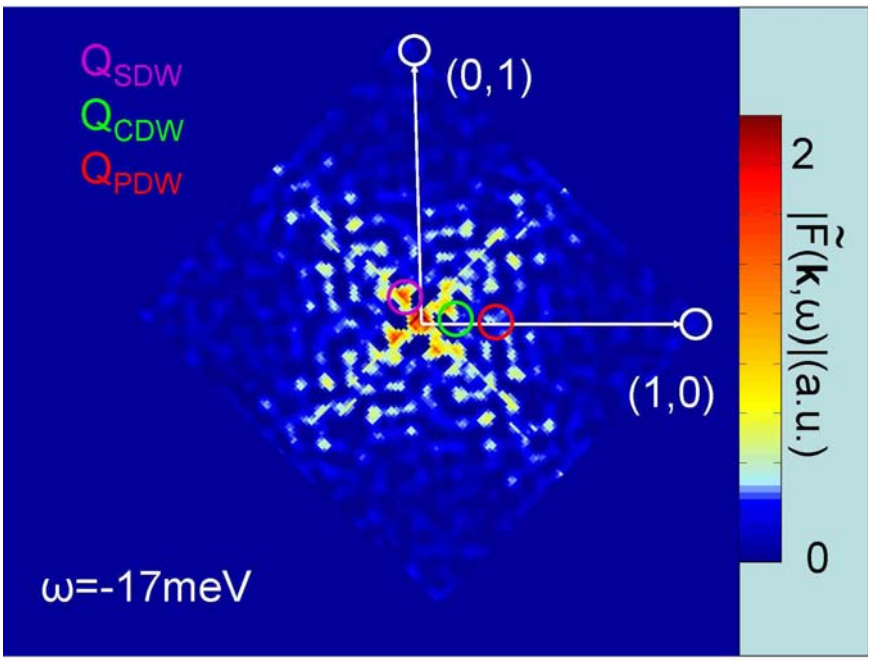

Figure B.13: $\tilde{F}$(**k**,ω=-17meV,H=5T)

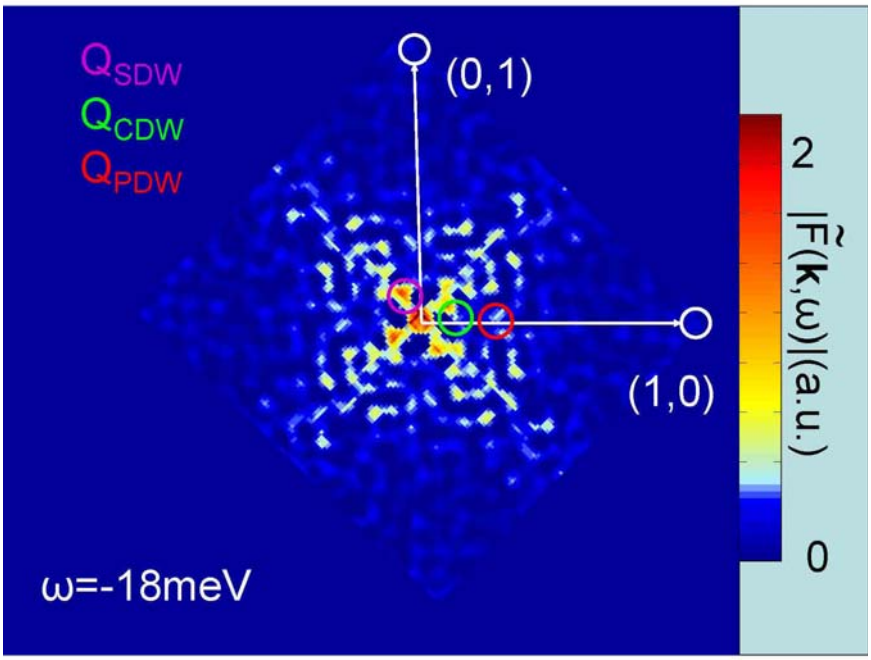

Figure B.14: $\tilde{F}(\mathbf{k},\omega$=-18meV,H=5T)

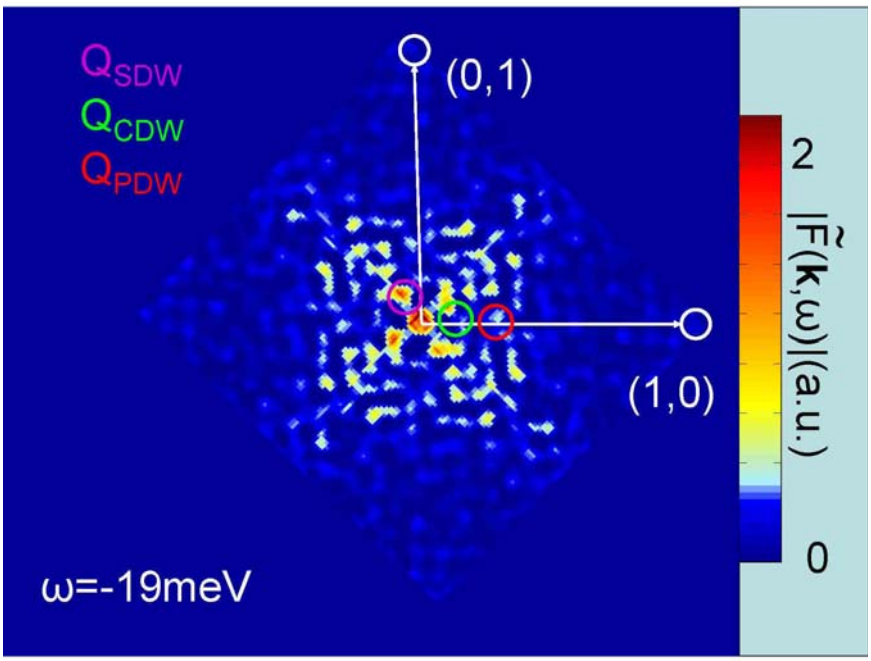

Figure B.15: $\tilde{F}(\mathbf{k},\omega$=-19meV,H=5T)

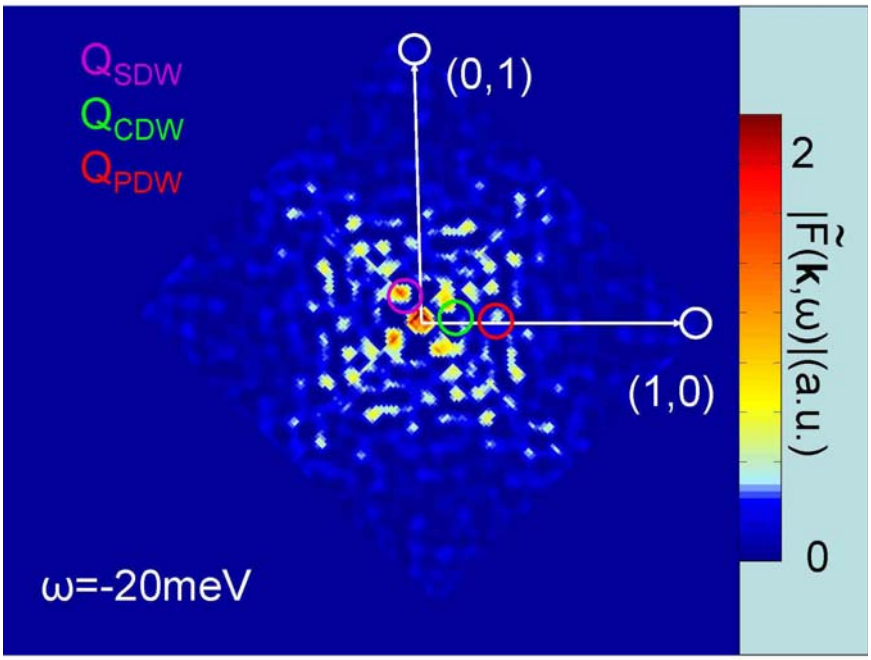

Figure B.16: $\tilde{F}$(**k**,ω=-20meV,H=5T)

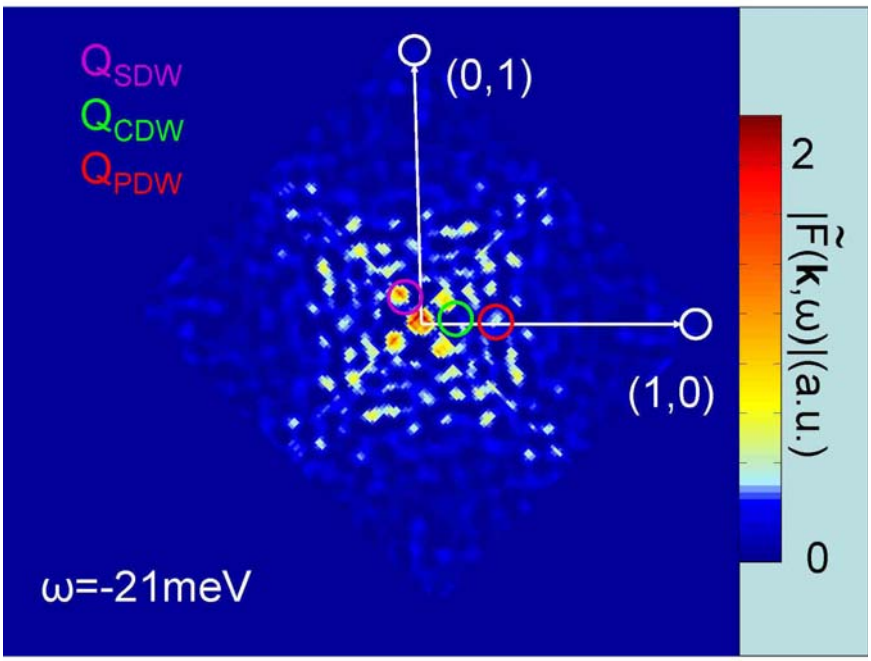

Figure B.17: $\tilde{F}$(**k**,ω=-21meV,H=5T)

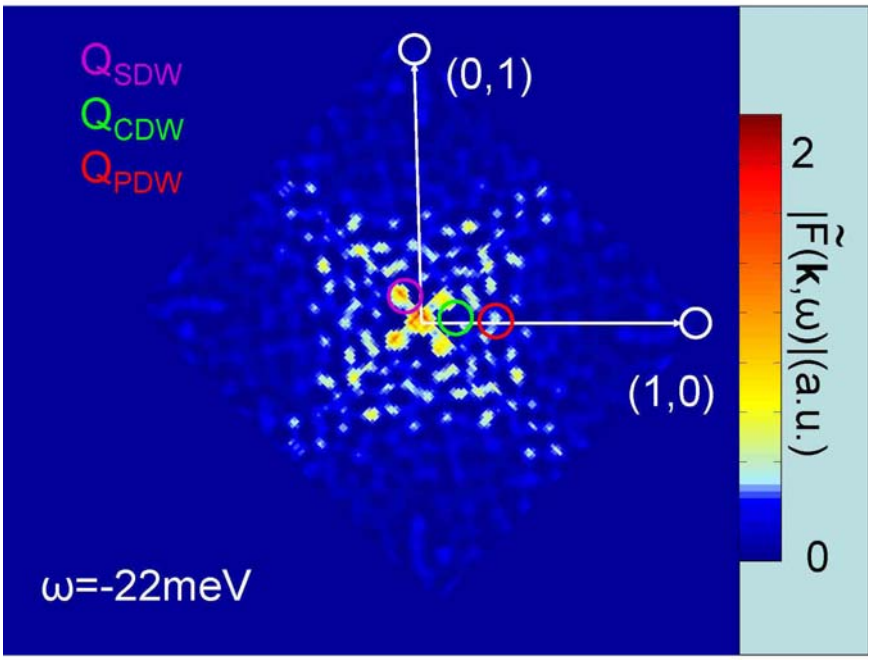

Figure B.18: $\tilde{F}(\mathbf{k},\omega$=-22meV,H=5T)

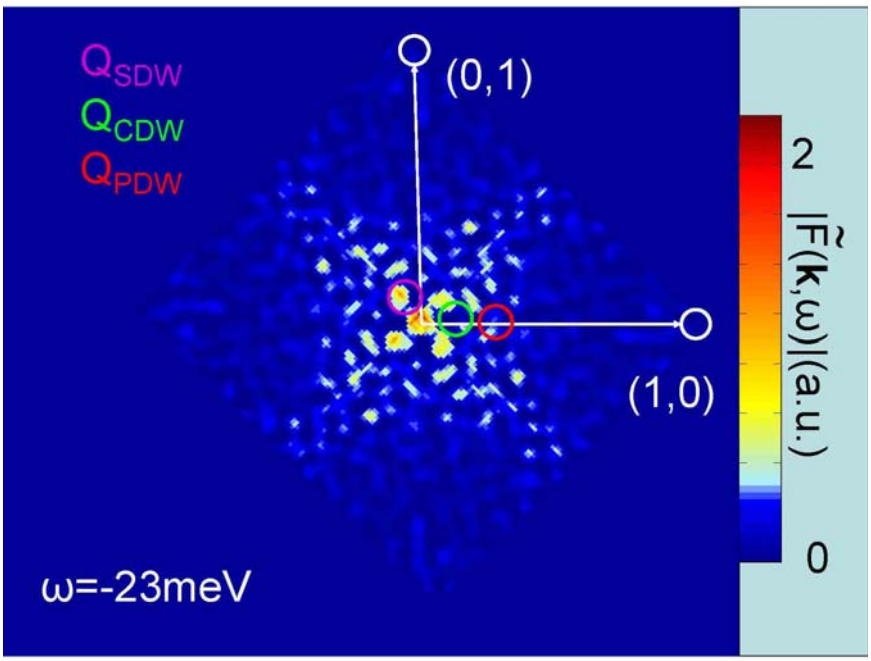

Figure B.19: $\tilde{F}(\mathbf{k},\omega$=-23meV,H=5T)

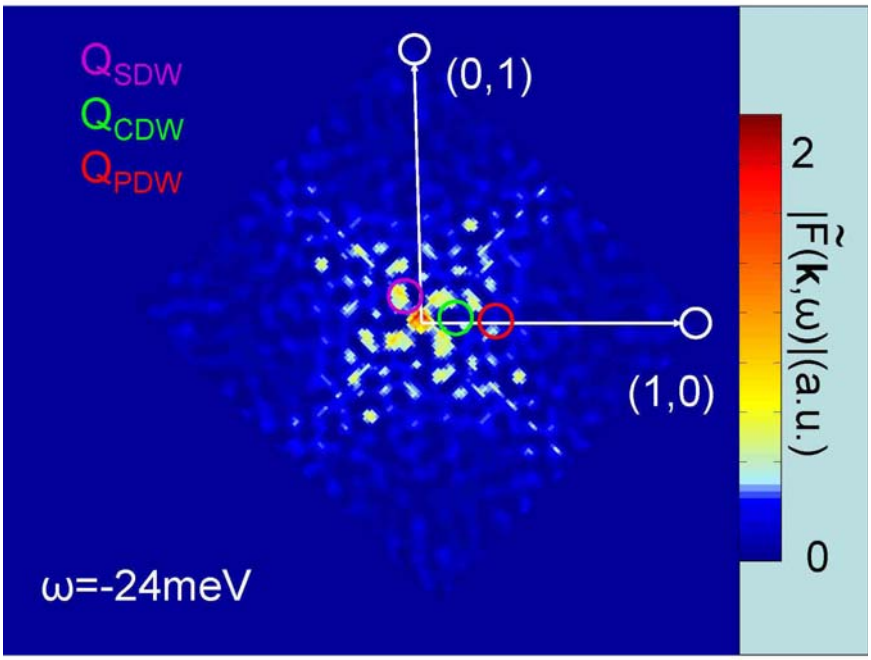

Figure B.20: $\tilde{F}(\mathbf{k},\omega$=-24meV,H=5T)

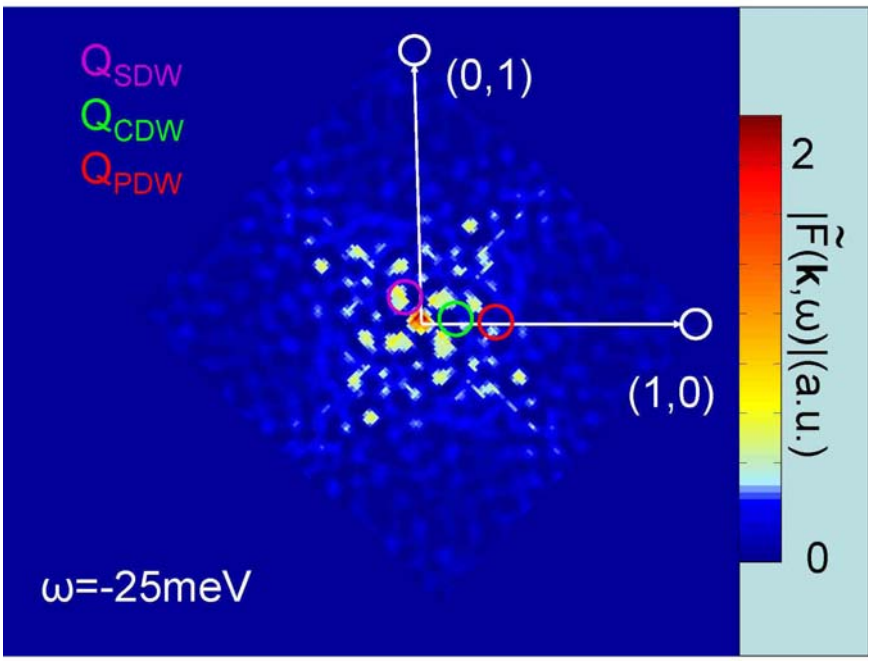

Figure B.21: $\tilde{F}(\mathbf{k},\omega$=-25meV,H=5T)

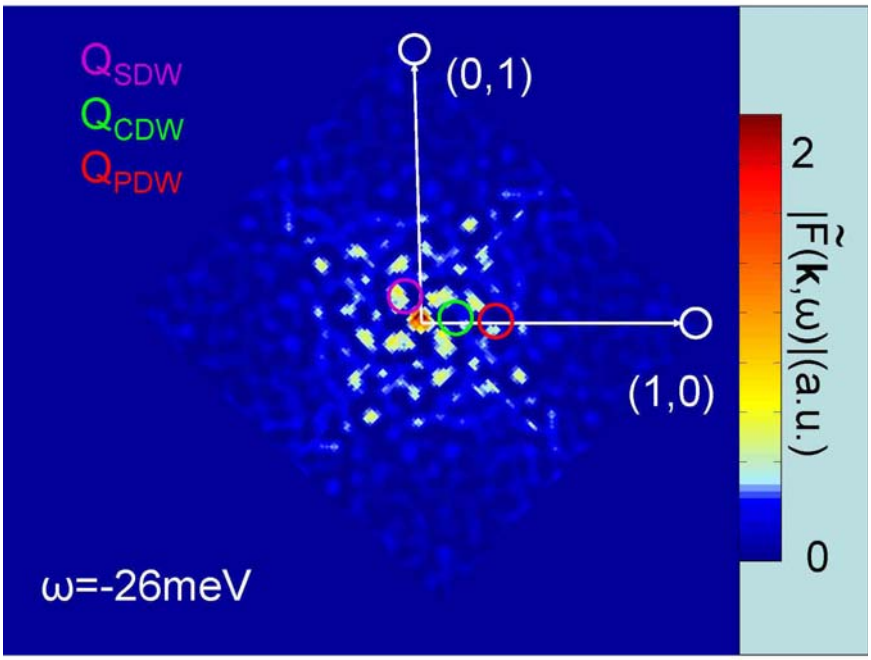

Figure B.22: $\tilde{F}(\mathbf{k},\omega$=-26meV,H=5T)

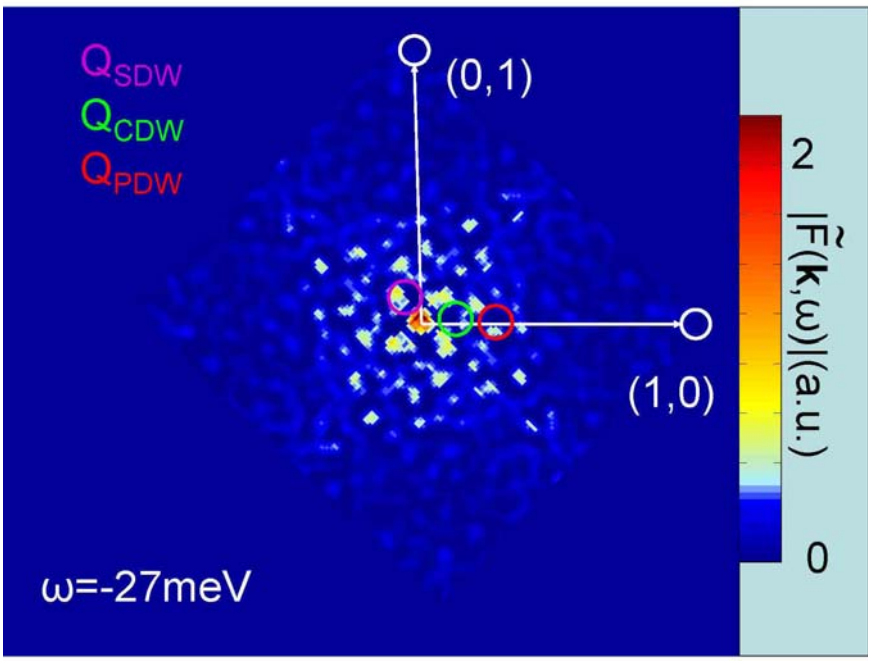

Figure B.23: $\tilde{F}(\mathbf{k},\omega$=-27meV,H=5T)

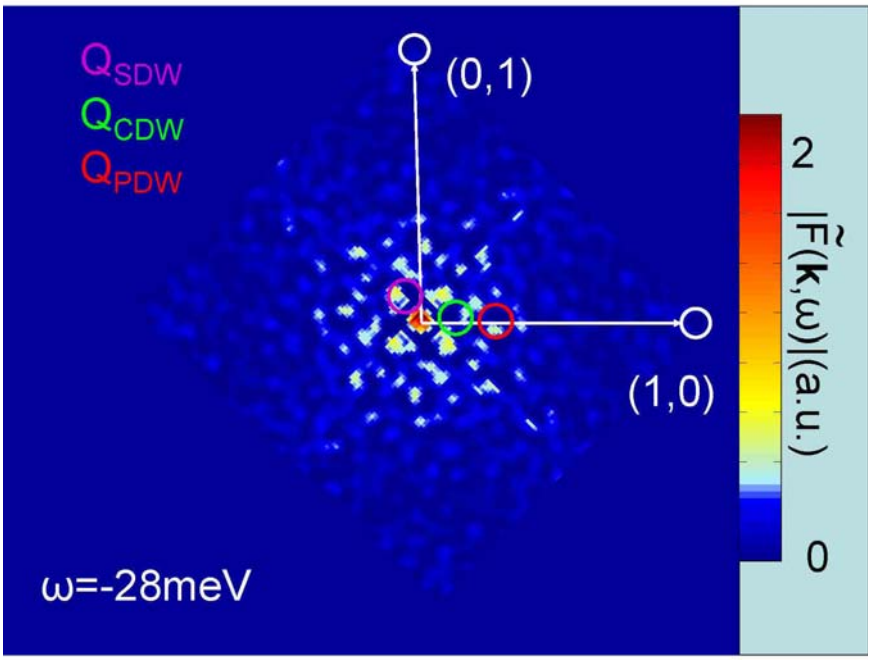

Figure B.24: $\tilde{F}(\mathbf{k},\omega$=-28meV,H=5T)

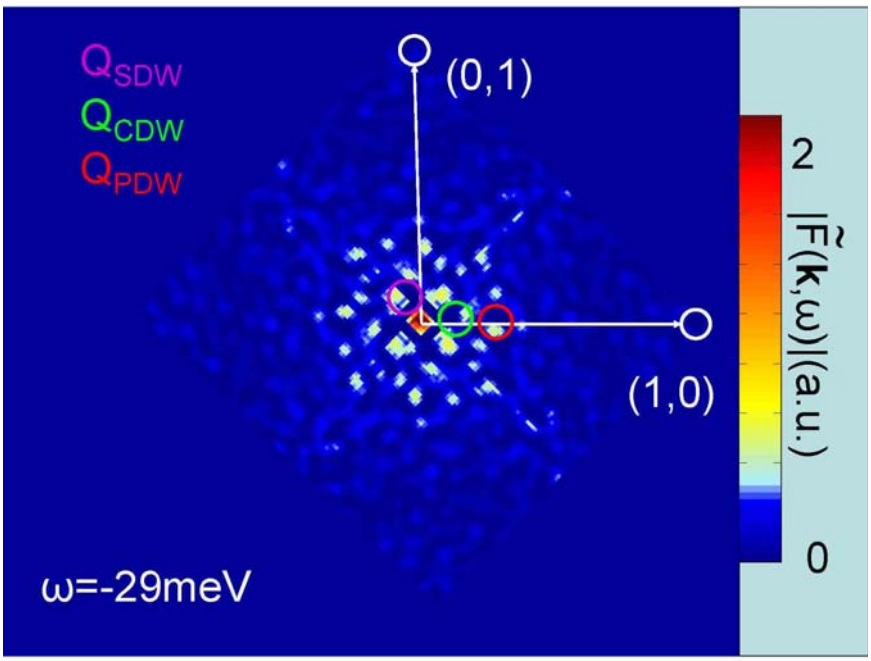

Figure B.25: $\tilde{F}(\mathbf{k},\omega$=-29meV,H=5T)

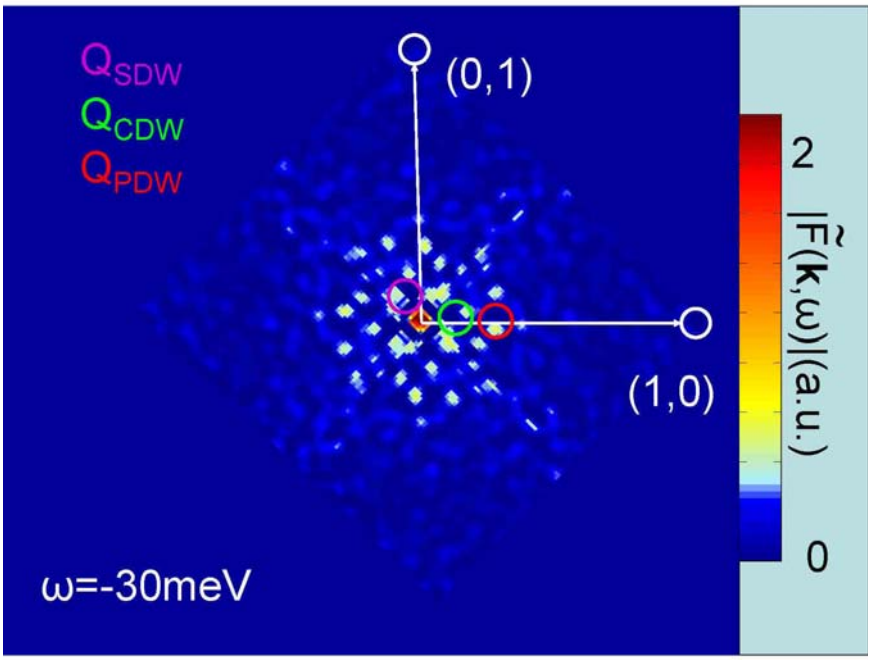

Figure B.26: $\tilde{F}$(**k**,ω=-30meV,H=5T)

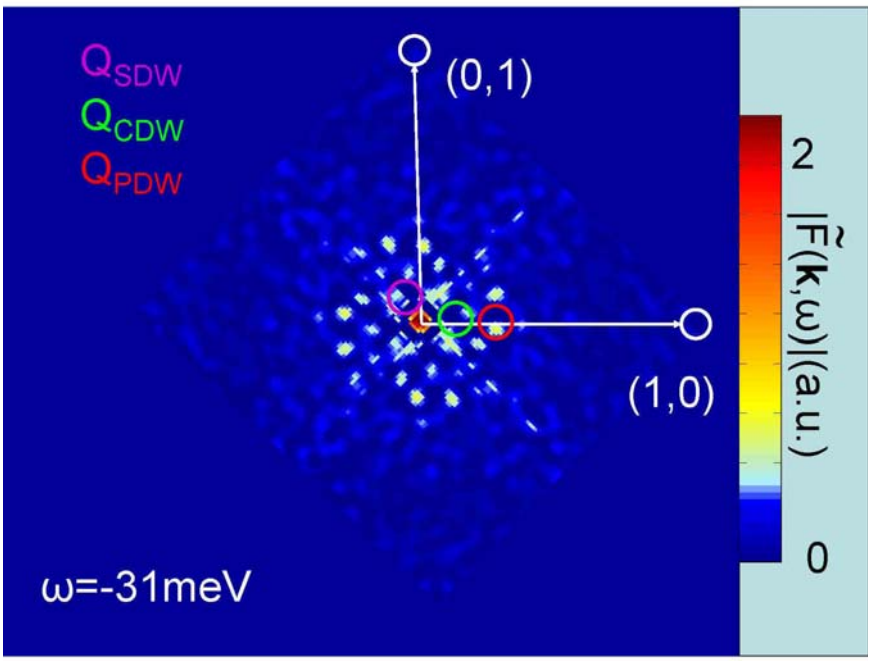

Figure B.27: $\tilde{F}$(**k**,ω=-31meV,H=5T)

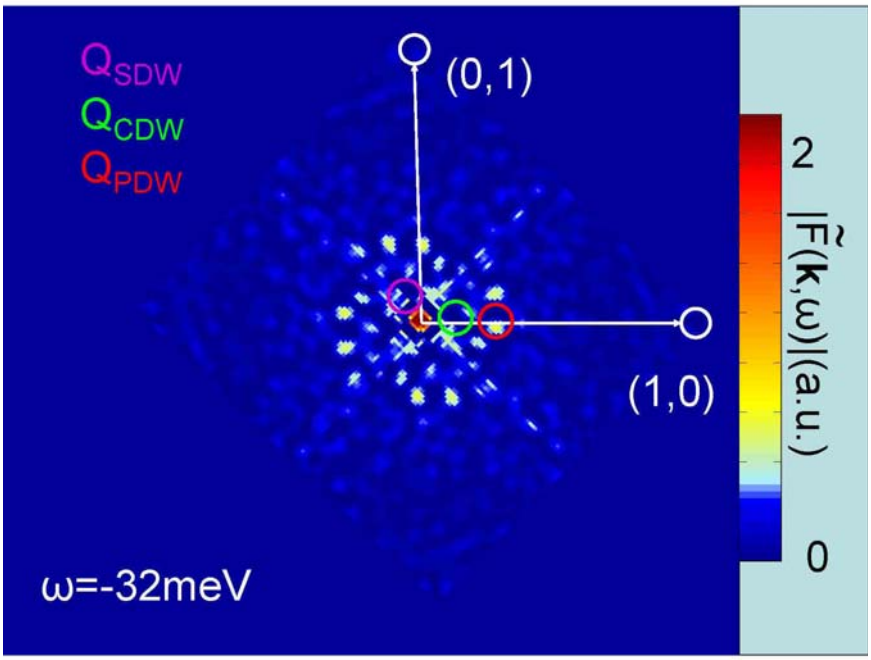

Figure B.28: $\tilde{F}$(**k**,ω=-32meV,H=5T)

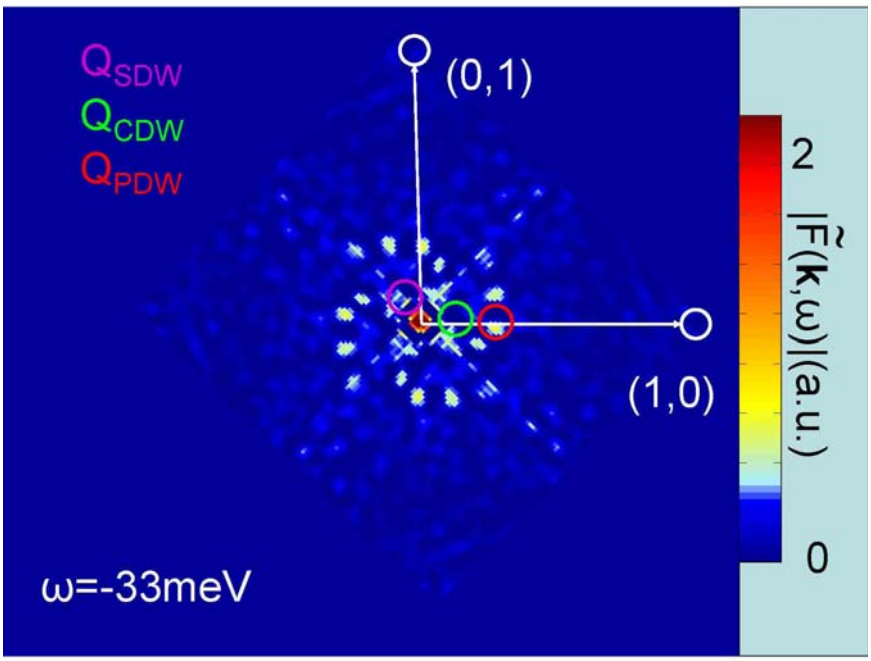

Figure B.29: $\tilde{F}$(**k**,ω=-33meV,H=5T)

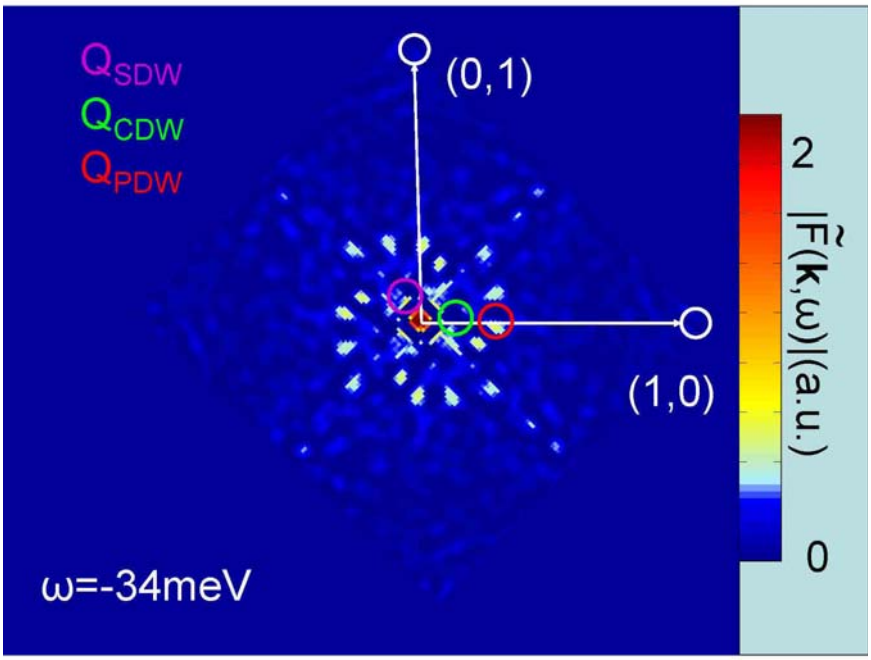

Figure B.30: $\tilde{F}(\mathbf{k},\omega$=-34meV,H=5T)

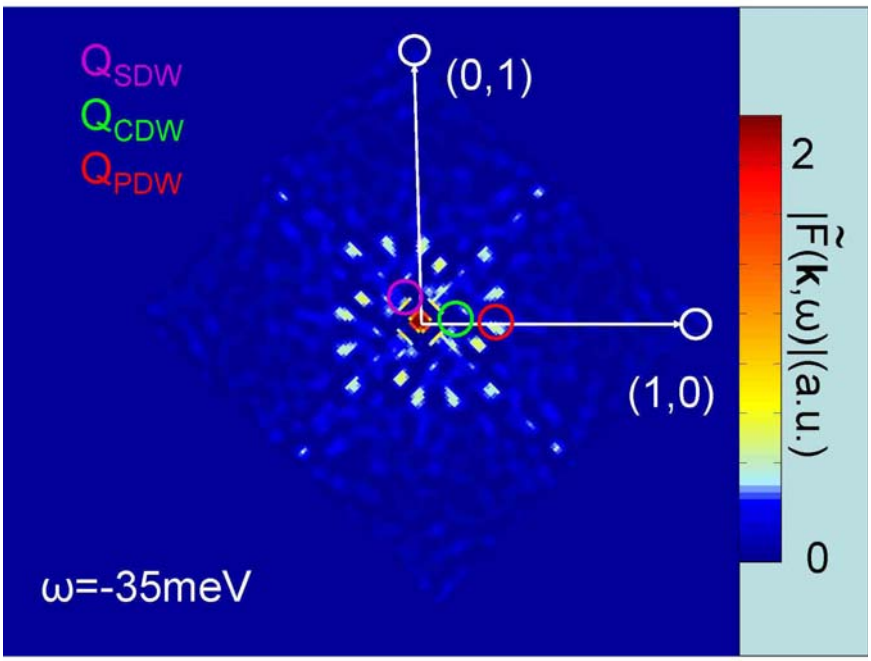

Figure B.31: $\tilde{F}(\mathbf{k},\omega$=-35meV,H=5T)

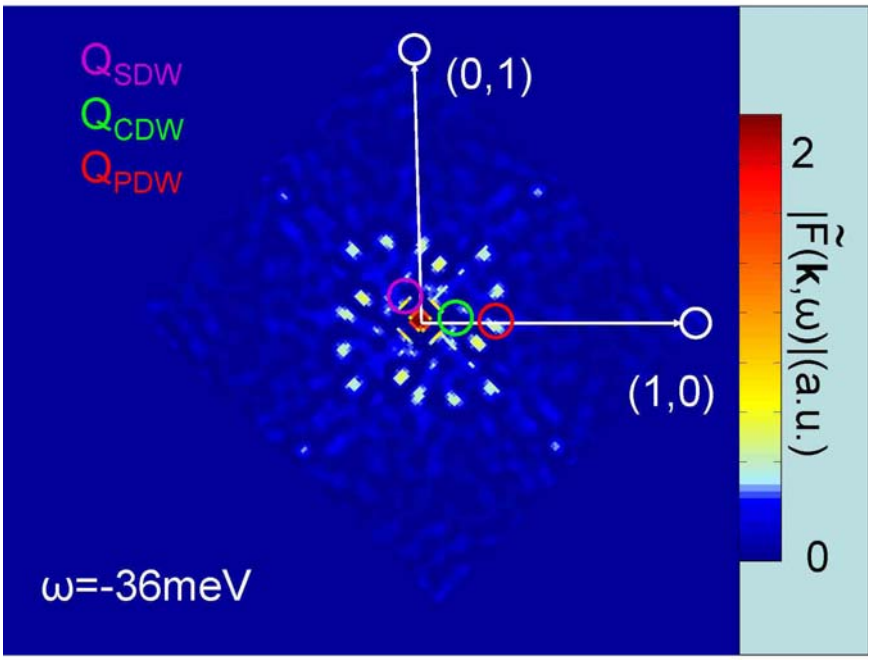

Figure B.32: $\tilde{F}(\mathbf{k},\omega$=-36meV,H=5T)

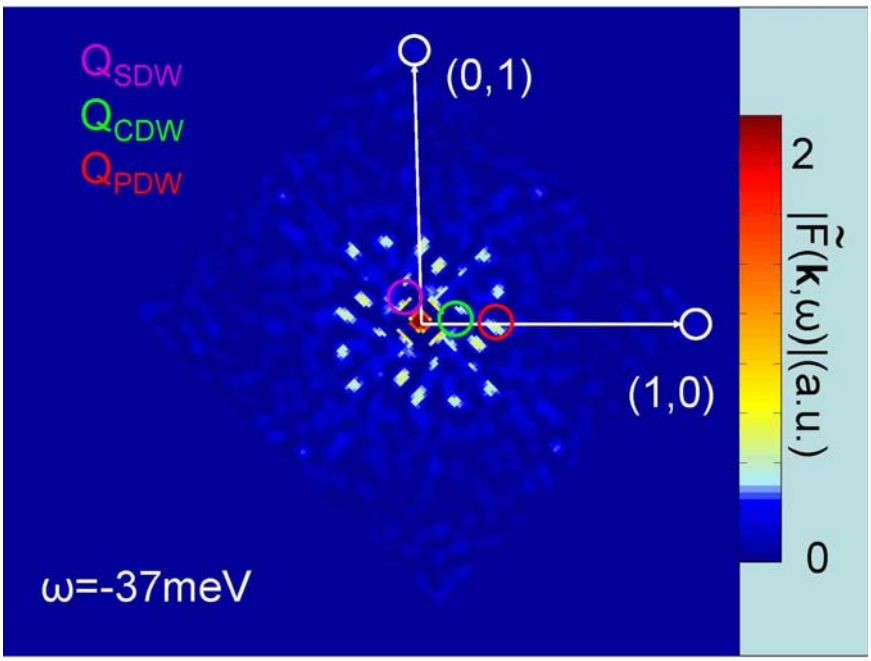

Figure B.33: $\tilde{F}(\mathbf{k},\omega$=-37meV,H=5T)

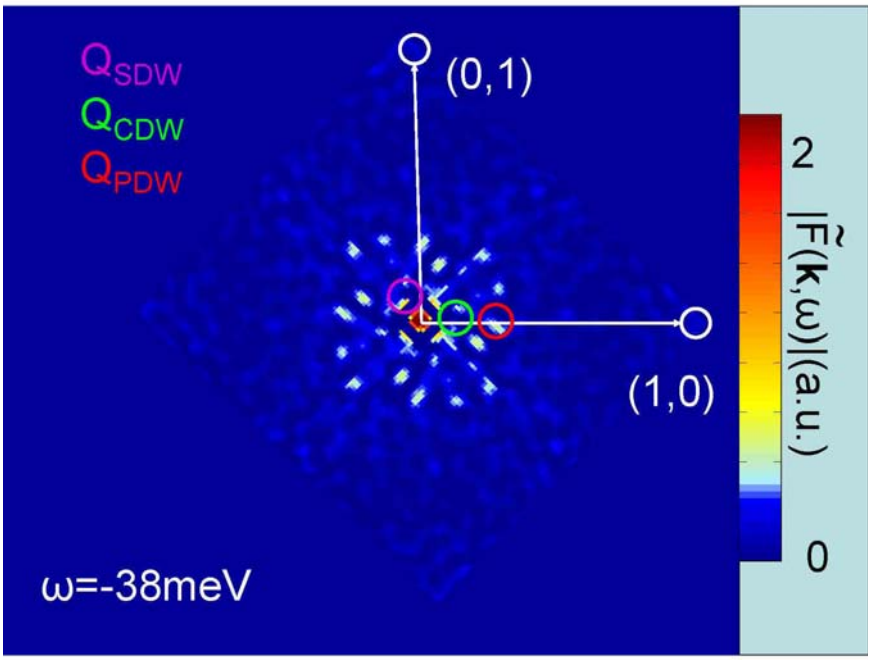

Figure B.34: $\tilde{F}(\mathbf{k},\omega$=-38meV,H=5T)

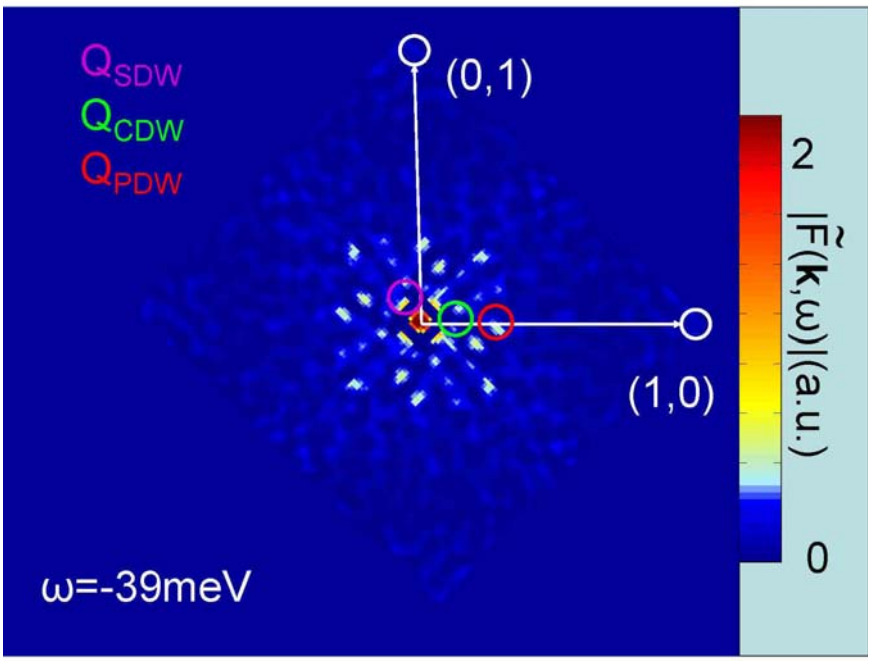

Figure B.35: $\tilde{F}(\mathbf{k},\omega$=-39meV,H=5T)

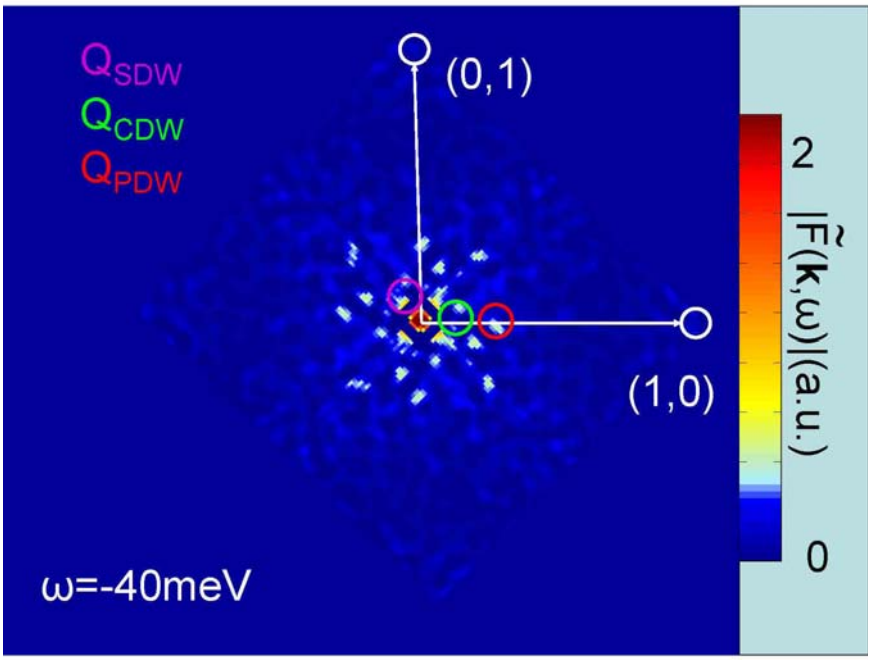

Figure B.36: $\tilde{F}(\mathbf{k},\omega$=-40meV,H=5T)

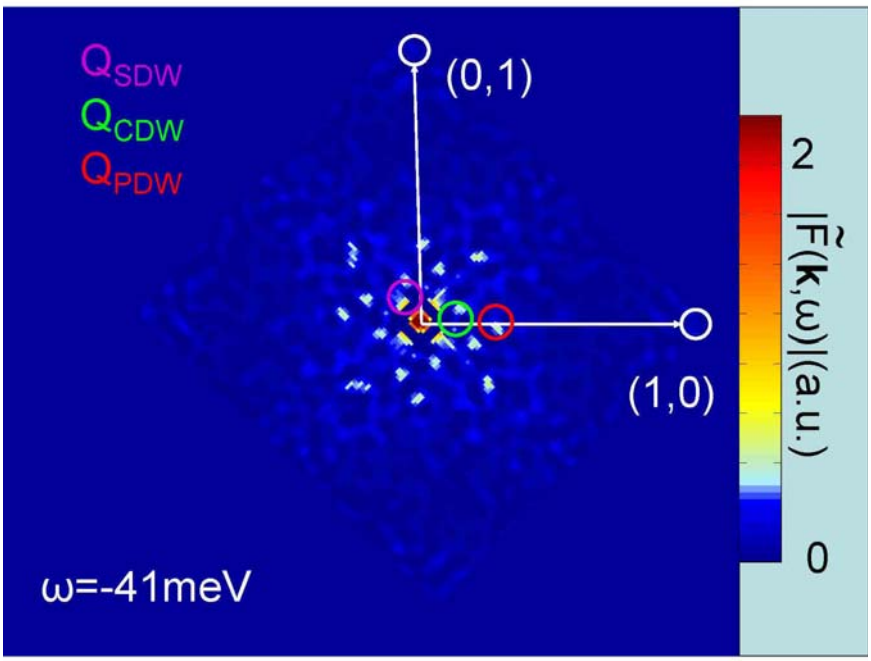

Figure B.37: $\tilde{F}(\mathbf{k},\omega$=-41meV,H=5T)

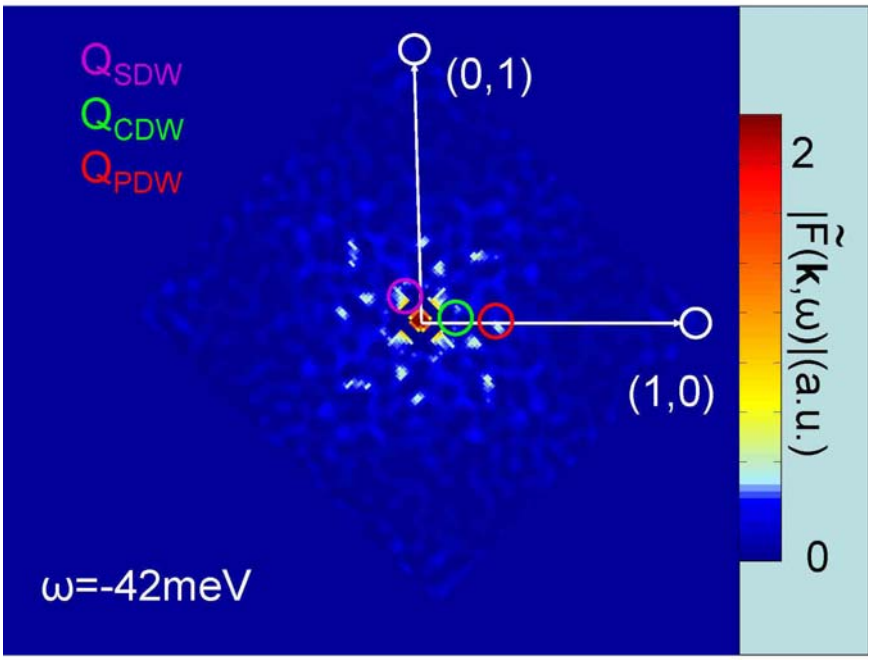

Figure B.38: $\tilde{F}(\mathbf{k},\omega$=-42meV,H=5T)

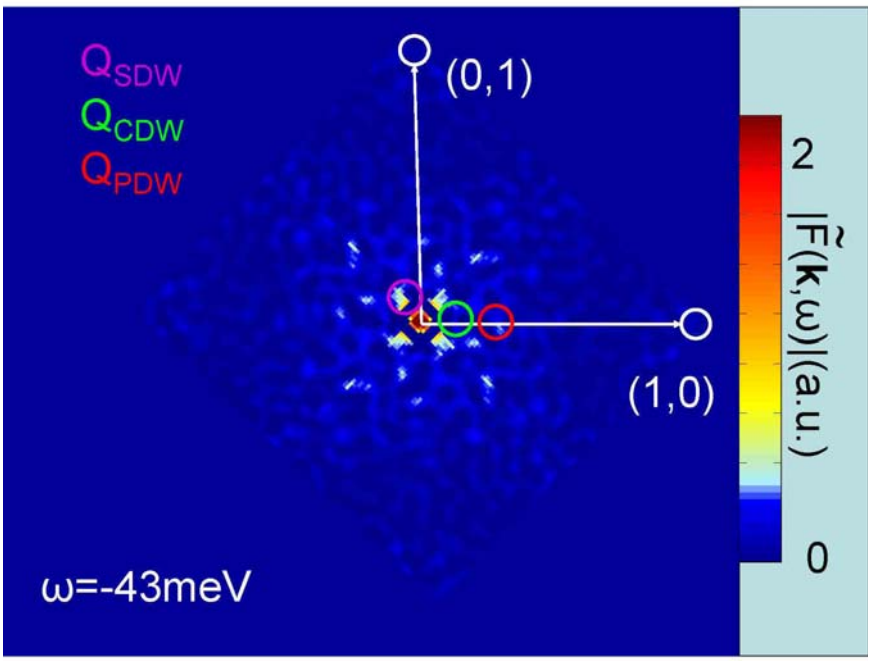

Figure B.39: $\tilde{F}(\mathbf{k},\omega$=-43meV,H=5T)

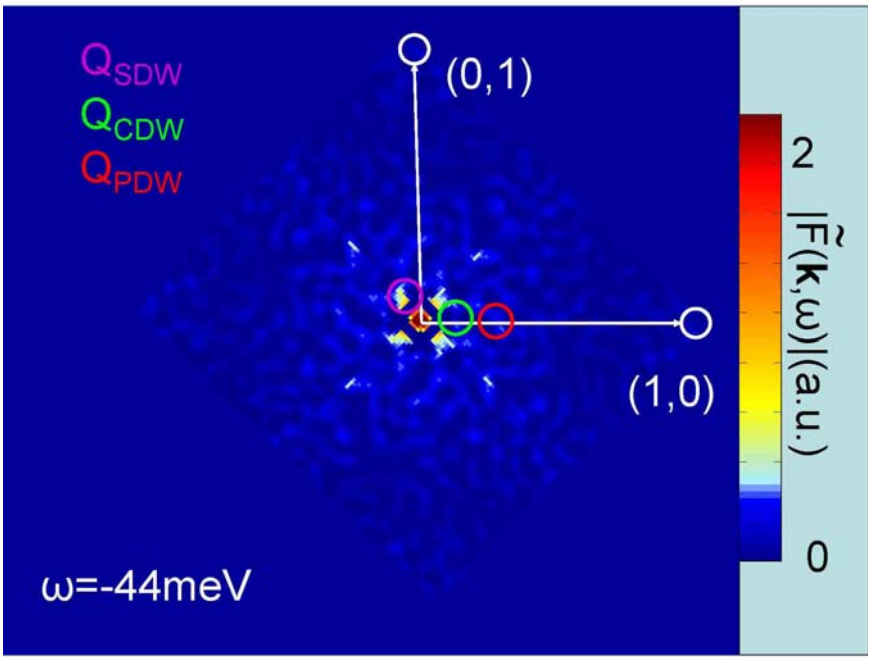

Figure B.40: $\tilde{F}(\mathbf{k},\omega$=-44meV,H=5T)

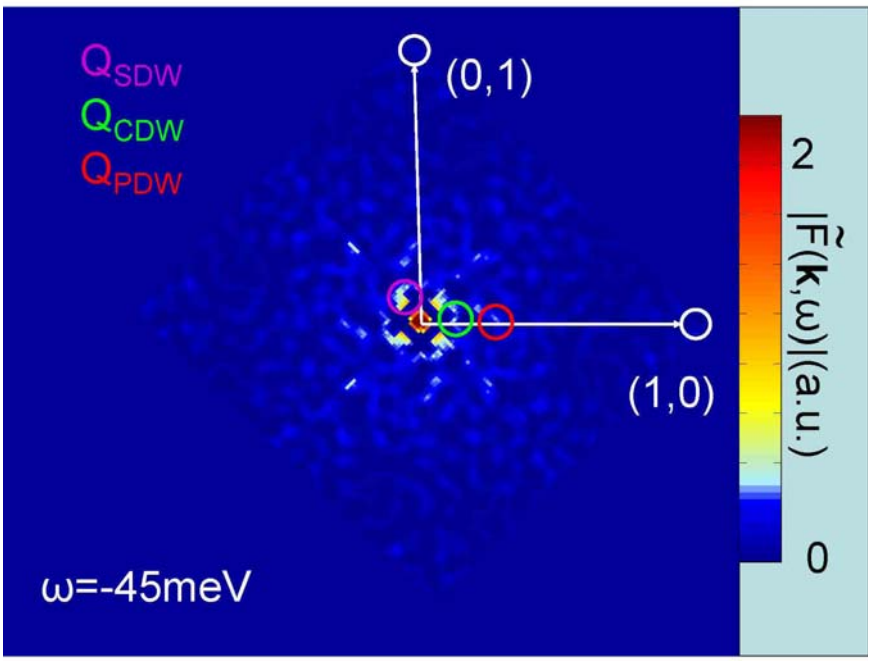

Figure B.41: $\tilde{F}(\mathbf{k},\omega$=-45meV,H=5T)

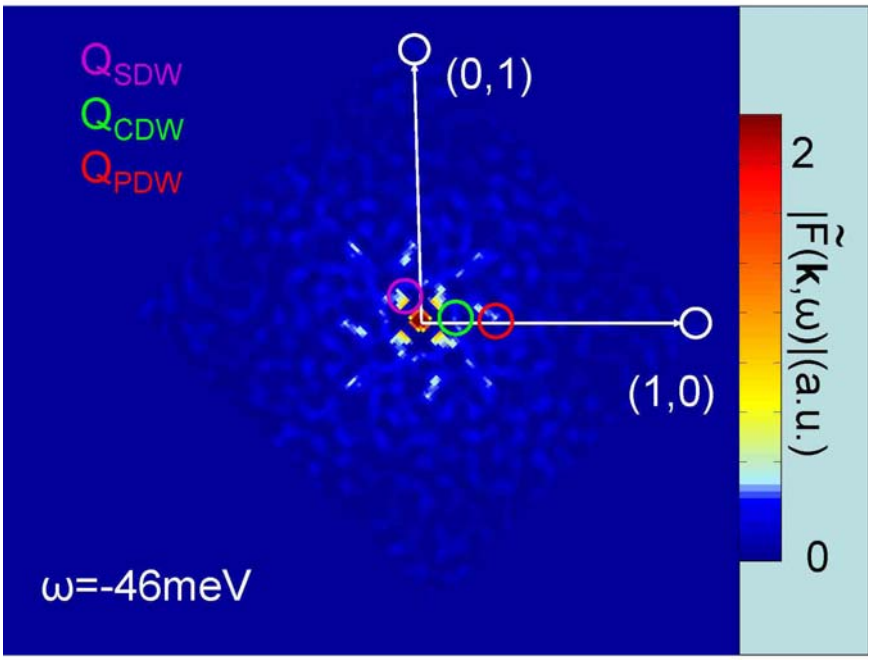

Figure B.42: $\tilde{F}(\mathbf{k},\omega$=-46meV,H=5T)

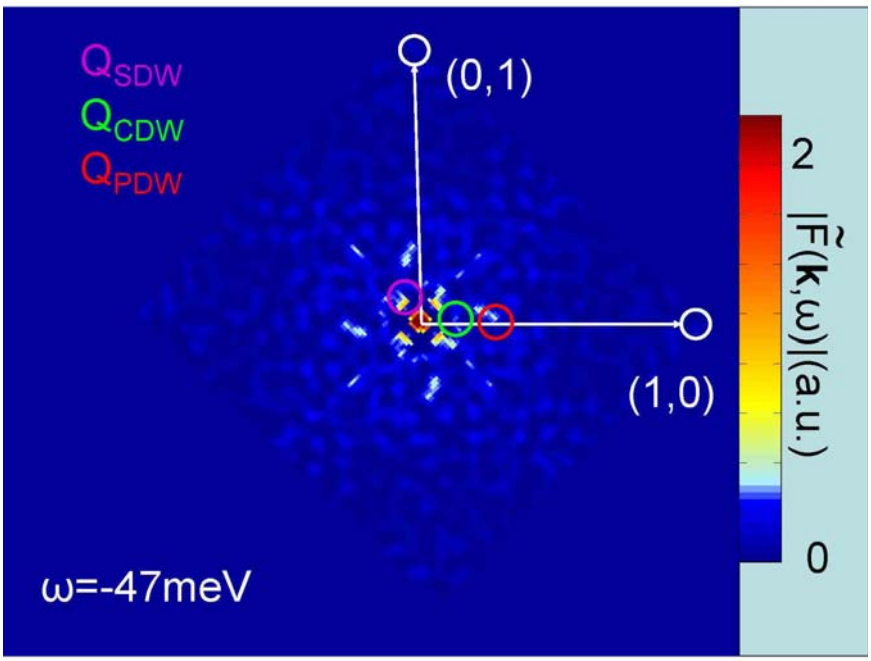

Figure B.43: $\tilde{F}(\mathbf{k},\omega$=-47meV,H=5T)

Appendix C

Progress toward development of a cryogenic scanning tunneling microscope/scanning electron microscope (STM/SEM)

Many challenges arise when performing scanning tunneling microscopy (STM) studies on inhomogeneous samples because of the limited maximum field-of-view ($\sim 10 \times 10\ \mu m^2$) and slow scanning speed of STM for typical STM designs ($\sim$ minutes or hours to scan the entire maximum field-of-view). However, the atomic scale resolution constant-current imaging and spectroscopy capabilities of STM provide a vital tool for characterizing local surface properties of materials and devices at the atomic scale. In contrast, scanning electron microscopy (SEM) offers fields-of-view ranging from approximately $100 \times 100\ nm^2$ up to $1 \times 1\ mm^2$ and can perform entire field-of-view scans in less than a second under ideal circumstances. However, the analytical characterization capabilities of SEM are limited to a maximum resolution of $\sim$10nm. A combined STM/SEM is expected to reduce the time for locating nano-scale devices and samples of interest within a large area of material from the order of weeks to hours. Additionally, an STM/SEM would allow characterization of samples using both STM and SEM techniques and would enable new studies to be performed by combining both techniques simultaneously. In this Appendix, we present progress to date on the development of a cryogenic scanning tunneling/scanning electron microscope (STM/SEM) for the Kavli Nanoscience Institute at Caltech. The cryogenic STM/SEM is expected to facilitate effective investigations of

complicated nano-scale features over an extended spatial area using both STM and SEM techniques.

C.1 Overview and ultra-high vacuum (UHV) components

The cryogenic STM/SEM is designed to perform all operations under ultra-high vacuum (UHV) conditions and follows a design for UHV cryogenic STM operation similar to Ref. [193]. An overview illustration of the instrument is shown in Fig. C.1. As shown in the figure, analysis using both STM and SEM will be performed in the main analysis chamber of the UHV arrangement. The SEM electron column[1], for generating the electron beam for SEM imaging and analysis, and the detector will be inserted into angled conflat flanges near the top of the main analysis chamber to allow SEM imaging and analysis to be performed in the main analysis chamber. An XYZ and rotary manipulator (XYZR)[2] is mounted to the top of the main analysis chamber[3], and a cryo-cooler[4] is mounted through the middle of the XYZR manipulator and attached through a 10" conflat flange in order to provide a cold stage, moveable stage for the STM. The STM head is attached to the end of the cryo-cooler and may be located within the line-of-sight of the SEM column and detector, using the XYZR manipulator, for simultaneous STM and SEM analysis in the main analysis chamber. The XYZR manipulator can also position the STM in the lower section of the main analysis chamber for tip and sample exchange.

The SEM electron column used is a UHV compatible Schottky emission electron column with a variable beam energy from 1keV to 25keV. It is designed to fit into a 4.5" conflat flange on the STM/SEM with a working distance of 2.55". An additional 4.5" conflat flange is provided on the main analysis chamber to put the SEM at working distance of 0" relative to the centerline of the main analysis chamber. A custom flange can then be built and added to this flange to provide another working distance, in the event that a 2.55" working distance is inadequate for operation or if there is a clash of instrumentation. Detectors for backscattered and secondary electron emission will include

[1] FEI UHV Subsystem SEM, 2LE Schottky Emission Electron Column

[2] Omniax manipulator from VG Scienta, Inc. Simstep stepper motor and Simstep Motor controller for controlling XYZR motion also from VG Scienta, Inc.

[3] Custom chamber designed by the author and built by VG Scienta

[4] Helitran cryo-cooler from ARS, Inc.

an Everhart-Thornley detector for secondary electrons or a solid-state detector for backscattered electrons. More details on detector types may be found in Ref. [194].

Oxygen free high thermal conductivity (OFHC) thermal radiation shields[5] surround the STM and join it to the cold stages of the cryo-cooler. At the bottom of the main analysis chamber a wobble-stick is attached to provide in-vacuum motion in order to lower the OFHC radiation shields for STM tip or sample exchange. The STM/SEM analysis is performed in the top portion of the main analysis chamber with the OFHC thermal radiation shields raised, and the STM may be lowered to the bottom portion using the XYZ and rotary manipulator to lower the thermal radiation shields and exchange samples or tips. More details of the cryogenic operation and exchange of tips and samples are presented more fully in Section C.4.

An ion pump[6], turbomolecular pump[7], and scroll pump[8] serve to pump out the STM/SEM chambers. To reach UHV conditions, the turbomolecular, the scroll pump, and the ion pump will be used to initially evacuate the main analysis chamber. Upon reaching UHV vacuum conditions, the turbomolecular pump and scroll will be disengaged, and the ion pump will maintain UHV during sensitive measurements using the STM and SEM. The ion pump will also be used to maintain UHV conditions in the main analysis chamber while the turbomolecular and scroll pump evacuate the load-lock chamber for introducing tips and samples for exchange. Gate valves[9] are installed to allow isolation of the pumps from the main analysis chamber as needed. An ion gauge and Pirani gauge[10] will be used for measurements of the pressure near the STM/SEM from atmospheric pressure to UHV conditions.

A load-lock chamber consisting of a six-way cross, optical viewports, 6" gate valve[11], a vacuum carousel[12] for holding tips and samples to be exchanged, and a linear, rotary manipulator[13] for performing exchange of tips and samples is attached to the side of the main analysis chamber. The

[5]Constructed from OFHC copper, 0.032" thick
[6]LION 40 Ion Pump with 2 ports, SafeLION Feedthrough and Bakeout heater purchased from Kurt J. Lesker Co.
[7]TMU 071YP TurboDrag Pump with TC 100 on-board electronics purchased from Pfeiffer Vacuum
[8]XDS5 Scroll Pump wired for 115V purchased from Kurt J. Lesker Co.
[9]Two 4.5" copper bonnet gate valve purchased from Kurt J. Lesker
[10]IGC3 ion gauge controller with Pirani Module and adaptor cable purchased from VG Scienta, Inc.
[11]Softshut 6" UHV Gate Valve purchased from VG Scienta, Inc.
[12]Rotary, linear direct drive from MDC Vacuum
[13]Rotary Linear Magnetic Drive, 24" linear travel, 2 3/4" ODCF purchased from VG Scienta, Inc.

load-lock chamber is evacuated with the large gate valve, that separates the load-lock chamber and main analysis chamber, closed ([7] in Fig. C.1), and tips or samples are introduced into the main analysis chamber using the linear, rotary manipulator.

C.2 Design of the STM

The STM for the STM/SEM is designed similarly to the STM described in Chapter 3; however, significant modifications have been made to further optimize the performance at cryogenic temperatures and to reduced the susceptibility of the STM to vibrations. The design of the molybdenum STM head is shown as a 2D image of the solid model in Fig. C.2a and in actuality in Fig. C.2b.

The STM incorporates XY and Z coarse-motion stages with the same working principle and design as described in Fig. 3.2, 3.5, and 3.6. Similarly, the piezoelectric tube scanner that provides fine STM tip scanning motion is the same type of piezo tube scanner as described in Fig. 3.3.

One difference from the previous design is that the body of the STM on the STM/SEM is made out of molybdenum, instead of Macor[14]. An advantage of a molybdenum STM body is that it has more mass ($\sim$ 0.445kg) than a Macor STM body($\sim$ 0.100kg). The larger mass leads to a lower resonant mechanical frequency of the STM head when suspended from the rest of the STM/SEM instrumentation and less susceptibility to mechanical vibrations in general. Further, a molybdenum body will have a larger thermal mass than a similar head made out of Macor, and the enhanced thermal mass will reduce temperature fluctuations during STM measurements. In addition, a molybdenum body, compared to a Macor body, will have a higher thermal conductivity and a smaller thermal gradient between the cold stage of the cryo-cooler and the STM tip and sample stage. Finally, the thermal contraction/expansion coefficient of molybdenum is comparable to that of piezoelectric material, which is ideal for constructing an STM stage.

Due to the fact that the STM body is made out of molybdenum, wires and electrical connections must be electrically isolated from the molybdenum body. Wires were insulated from the STM body

[14]Macor is a machineable ceramic available from Corning Inc.

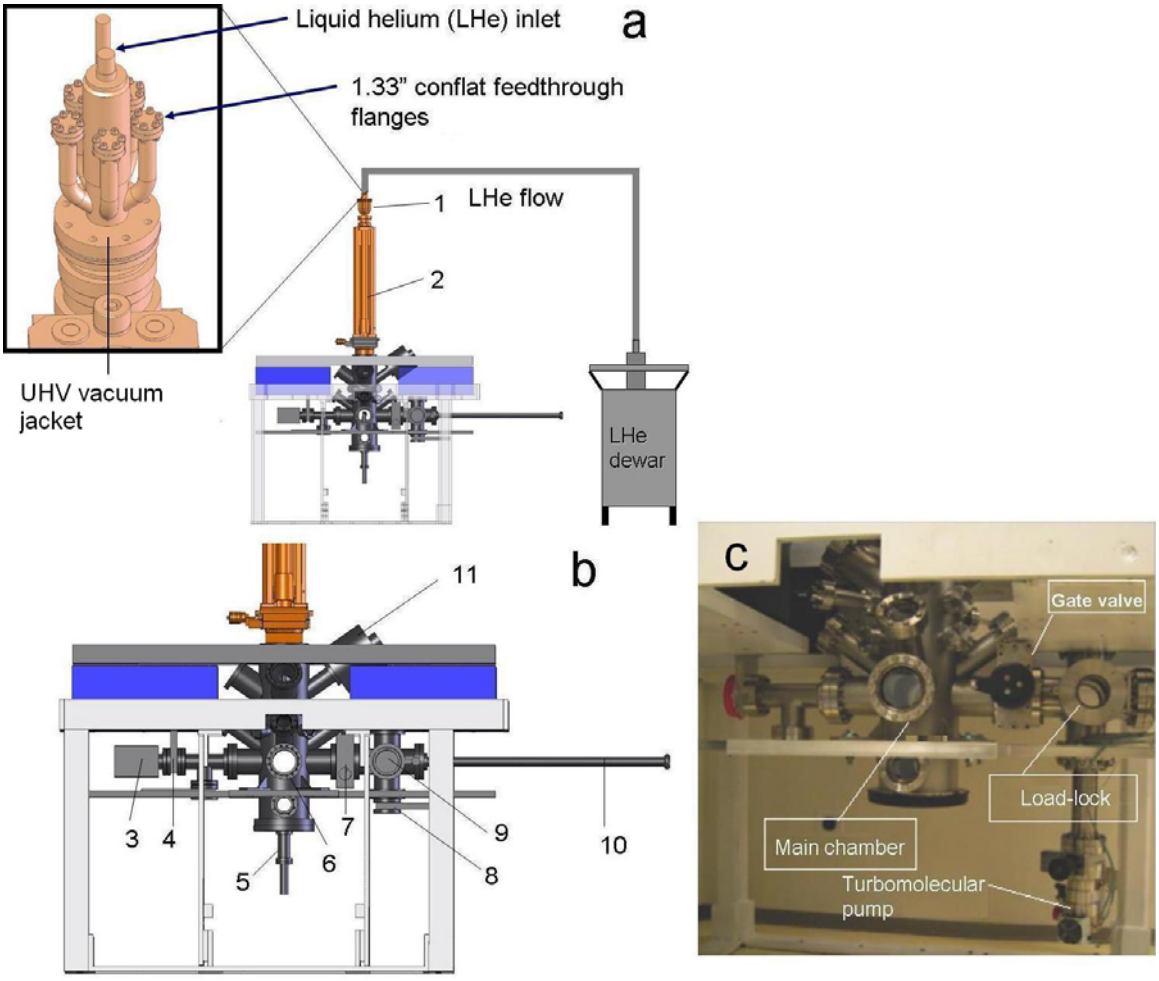

Figure C.1: Schematic illustration of the cryogenic STM/SEM: [1]–Helitran cryo-cooler, [2] Omniax XYZ and rotary (XYZR) manipulator, [3]–LION 40 Ion pump, [4]–Gate valve to isolate ion pump, [5]–Wobble stick, [6]–Main analysis chamber, [7]–Large gate valve separating the load-lock chamber and main analysis chamber, [8]–Gate valve for the turbomolecular pump and scroll pump, [9]–Load-lock door and six way cross for loading tips and samples onto the vacuum carousel, [10]–Linear, rotary manipulator for tip and sample exchange, [11]–UHV 2LE SEM electron column. (a) Schematic overview of the cryogenic STM/SEM system showing a liquid helium dewar attached to the cryo-cooler. Liquid helium flows through the cryo-cooler. The cryo-cooler is designed so that bubbling of liquid helium (LHe) during flow is eliminated in order to reduce vibrations. Five 1.33" conflat flanges are fed through a UHV vacuum jacket along with cryo-cooler cold tip, as shown in the expanded inset. Two BNC connectors and three 10-pin instrumentation electrical feedthrough connections are attached to these conflat flanges, along with wiring, to provide electrical connections to the STM head and temperature control on the STM head. In addition, the LHe dewar may placed onto an additional vibration isolation platform or hung from the ceiling using flexible attachments to further reduce coupling of vibrations to the STM/SEM. (b) Side-view close up model of the cryogenic STM/SEM. (c) Picture of the actual cryogenic STM/SEM.

using ceramic beads[15]. The piezoelectric stack connections were insulated from the molybdenum body by attaching alumina plates[16] to the underside of the pizeo stacks with epoxy[17]. The alumina plates were then attached to thin, square Shapal[18] plates, which were attached to the molybdenum using epoxy[19].

Another difference from the previous STM design is that the new STM body was machined out of a single piece of material so that the XY and Z coarse-motion stages are combined into a monolithic structure for XY and Z coarse-motion capability. In contrast, the STM described in Chapter 3 has separate XY and Z coarse motion stages that interlock together for combined XY and Z coarse-motion capabilities. It is expected that the monolithic design will reduce the susceptibility of the STM to mechanical vibrations between the XY and Z coarse-motion stages.

C.3 Vibration and acoustic noise isolation

The cryogenic STM/SEM required instrumentation to isolate the apparatus from vibrational and acoustic noise sources. Examples of noise sources present in the STM/SEM laboratory space include building vibrations and acoustic and vibrational noise from mechanical pumps. To isolate from these noise sources the STM/SEM was constructed on a concrete slab isolated from the rest of the laboratory, was loaded onto a spring loaded vibration isolation table, and was surrounded by thick plastic curtains to damp acoustic noise[20].

A concrete isolation slab, of dimension $5' \times 5.5'$, was constructed in the STM/SEM laboratory space to reduce the transmission of high frequency vibrations to the apparatus. The isolation slab was constructed by contractors, who dug a pit approximately $4'$. The pit was subsequently filled with compacted fill (95% compaction fill or greater) and topped with a 3" layer of sand to a net height of approximately $2'$. On top of the sand a $2'$ thick concrete slab was poured, and a sealant

[15] Fish-spline ceramic beads available from Kurt J. Lesker Co.
[16] 0.020" thick Superstrates manufactured by Coors Ceramic Company
[17] H74 epoxy purchased from Epotek
[18] Shapal is a machineable ceramic with slightly improved thermal conductivity compared to Macor and is available from Ceramic Substrates and Components Ltd.
[19] H74 epoxy
[20] Assembly and testing of the STM/SEM instrumentation for vibration and acoustic noise isolation was performed by the author and Guglielmo Lockhart. The work was performed by Guglielmo Lockhart as his SURF project during the summer of 2008

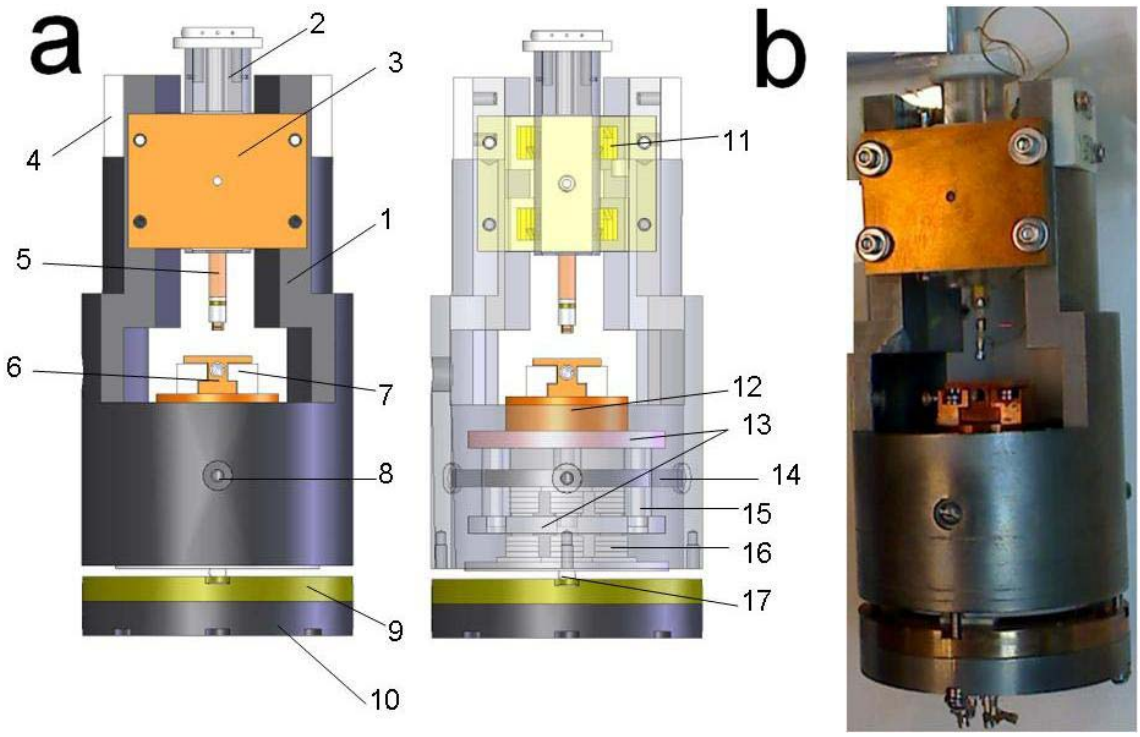

Figure C.2: Molybdenum STM head constructed and designed by the author. (Machining of parts was done by Nils Asplund and by the Physics Department Machine Shop staff under the direction of Richard Paniagua): (a) Left panel is a 2D image of the solid model (created in Solidworks CAD software). Right panel is a semi-transparent model of (a). [1]–Molybdenum body, [2]–Sapphire prism for Z coarse-motion stage, [3]–Copper-beryllium spring for adjusting tightness of piezo shear stacks on the sapphire prism for Z coarse-motion stage, [4]–Shapal electrical feedthrough for Z stage connections, [5]–Piezo tube scanner, [6]–Oxygen free high thermal conductivity (OFHC) removable copper stage, [7]–OFHC fixed copper stage fixed stage, [8]–Through hole for stainless steel (SS) screw to secure [14], [9]–Copper-beryllium spring for adjusting tightness of piezo shear stacks against the sapphire plates for the XY coarse-motion stage, [10]–Molybdenum bottom plate with Shapal electrical feedthrough stages for wiring to the XY coarse-motion stage piezo shear stacks, [11]–Piezo shear stack for Z stage, [12]–OFHC copper base for temperature sensors and heaters, [13]–Sapphire plates for XY coarse-motion stage, [14]–Molybdenum plate for supporting half of the XY stacks, [15]–Sapphire posts that link the two XY sapphire plates together, [16]–Piezo shear stack for XY stage, [17]–Sapphire ball for adjusting the the tightness of the XY coarse-motion stage piezo shear stacks. The functionality of the Z coarse-motion stage is described more fully in Fig. 3.5.

was filled between the isolation slab and the building floor grade. When finished, the concrete slab was flush with the floor of the lab space.

The entire STM/SEM apparatus is mounted to a vibration isolation table to reduce low frequency vibrations, and a 2D image of the solid model of the vibration isolation table arrangement is shown in Fig. C.3. The table is comprised of a steel support table, four vibration isolation platforms, and two aluminum plates. The steel table was designed by the author and built to specifications[21]. It approximately weighs one ton and sits directly on the aforementioned concrete isolation slab. The four vibration isolation platforms[22] are located on the four corners of the steel support table, and the 3"-thick top aluminum plate[23] sits directly on the vibration isolation platforms. The STM/SEM apparatus is mounted to the 3"-thick top plate, and a 1"-thick bottom aluminum plate[24] is suspended from the bottom of the STM/SEM apparatus. The bottom plate is designed to support additional STM/SEM parts and to add structures to support the UHV vacuum chamber parts. For instance, a support structure for the linear/rotary manipulator shown in Fig. C.1 is needed to prevent mechanical stress on this part, and a support structure can be machined and attached to the bottom aluminum plate.

The four vibration isolation platforms act like compression springs, and their effective spring constants are adjusted for optimal performance of the vibration isolation table. The spring constant of each vibration isolation platform may be adjusted using a simple crank mechanisms installed by the manufacturer until the table is supported vertically by the springs. Additionally, two horizontal sets of springs maintain the horizontal orientation of the STM/SEM. Ballast weights may be added to properly load the entire vibration isolation table[25]Upon proper tuning of the spring constants, the mechanical resonant frequency of the vibration isolation table in the vertical and horizontal directions is $\sim$0.5Hz.

To damp acoustic noise, thick plastic curtains on guide rails were installed around the entire

[21]Steel table built and welded together by CenterLine Welding, under the direction of Dale Giese
[22]BM-1 Benchtop Vibration Isolation platforms purchased from Minus K technology. Each platform can support up to 700 lbs
[23]3" aluminum plate designed by author and machined to specification by the D-M-E Co.
[24]1" aluminum plate designed by the author and machined by the D-M-E Co.
[25]The ballast weights consisted of concrete blocks encased and sealed in plastic boxes

STM/SEM apparatus, and the curtains were designed to prevent transmission of acoustic noise into the STM/SEM measurement area, as shown in Fig. C.3b. Additionally, the walls and doors of the STM/SEM room were designed with a Sound Transmission Class (STC) rating of approximately 45 to prevent the transmission of noise through the laboratory walls. (An STC rating is an ASTM International Classification standard rating that describes the ability of walls and doors to attenuate sound transmission for 16 standard frequencies from 125 Hz to 4000 Hz.)

The acoustic curtains were not found to significantly reduce acoustic noise levels inside the lab space. Calibrated microphone measurements using a condenser microphone and pre-amplifier did not detect a significant difference in acoustic noise levels with and without the acoustic curtains surrounding the instrumentation. The acoustic noise levels in the lab space are already expected to be low due to the STC 45 doors and walls, and it appears as though the curtains provide a negligible improvement. Additionally, an air vent is positioned within the space surrounded by the curtains. The air vent is likely the dominant noise source in the lab space, and curtains are ineffective against this acoustic noise source. Future measurements with the STM/SEM are needed to characterize the susceptibility of STM and SEM measurements to acoustic noise. It is possible that the current acoustic noise levels will not significantly affect actual STM/SEM measurements. Additional measures to reduce acoustic noise[26] may be implemented as needed.

To test the performance of the vibration isolation instrumentation, we performed accelerometer measurements of the vibration levels. The accelerometer measurements were performed by attaching an accelerometer to the support leg of the steel support table (no vibration isolation) and to the bottom aluminum plate of the vibration isolation table (with vibration isolation) for comparison. The results are shown in Fig. C.4. It is found that the vibration levels are significantly reduced over the frequency range up to 125 Hz when measured on the vibration isolation table compared to the steel support leg. Most notably, a significant vibration level above the noise level was detected at a frequency of 11Hz on the steel support leg. This frequency is likely the resonant building vibration frequency, and it is observed that this vibration level was significantly damped by the vibration

[26](a) Acoustic damping blankets could be installed in addition to the plastic curtains. Blankets may be purchased from All Noise Control, for example. (b) Bass absorbing traps could be added as well, and may be purchased from McMaster-Carr, for example

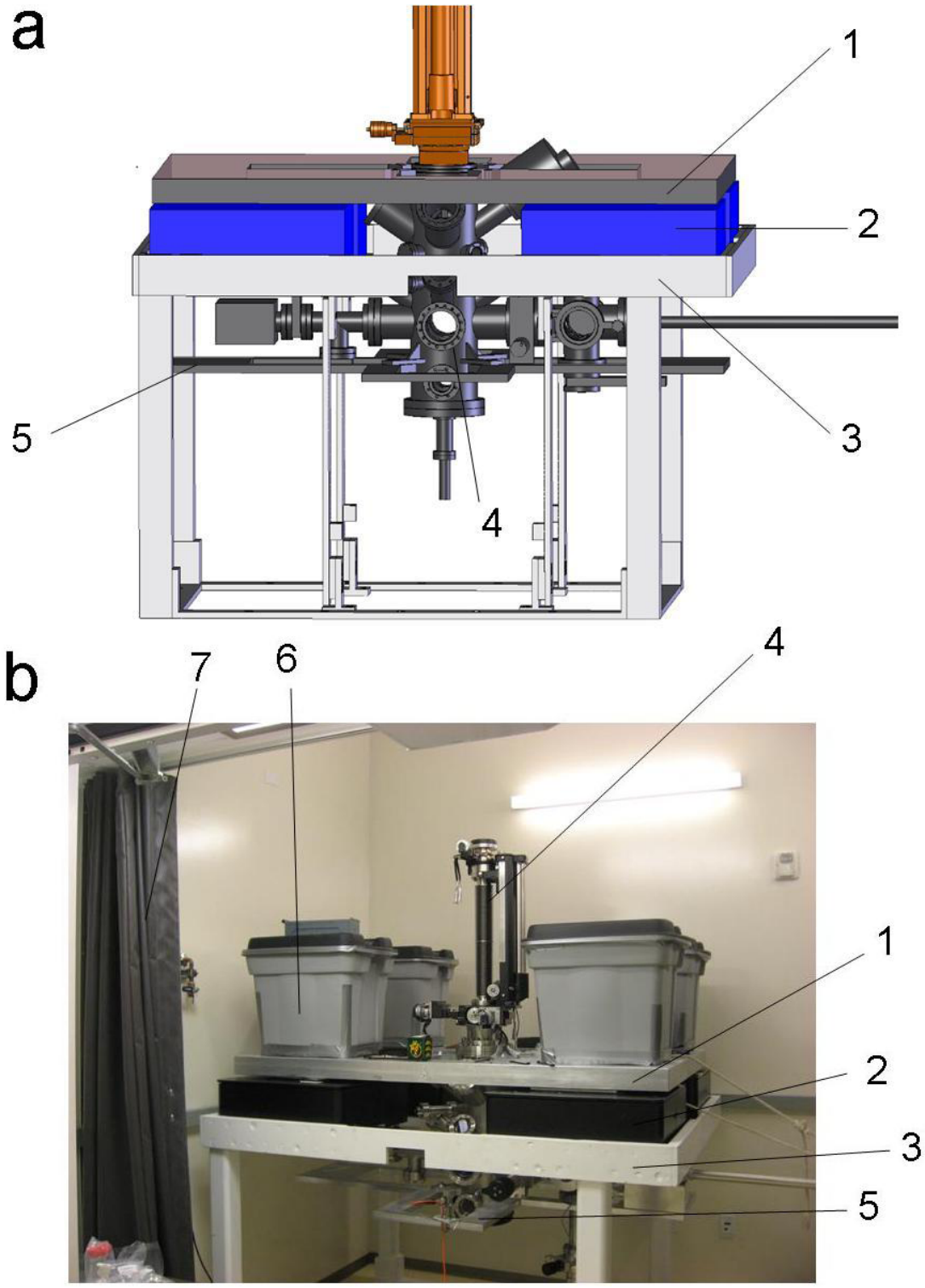

Figure C.3: Vibration isolation table for the cryogenic STM/SEM: [1]–Top 3"-thick aluminum plate, [2]–Vibration isolation spring platforms from Minus K Technology, [3]–Steel support table, [4]–STM/SEM apparatus main analysis chamber, [5]–Bottom 1"-thick aluminum plate. [6]–Ballast weights, [7]–Thick plastic curtains. (a) Two-dimensional image of the solid model of the vibration isolation table and STM/SEM. (b) Actual STM/SEM housed in its laboratory space.

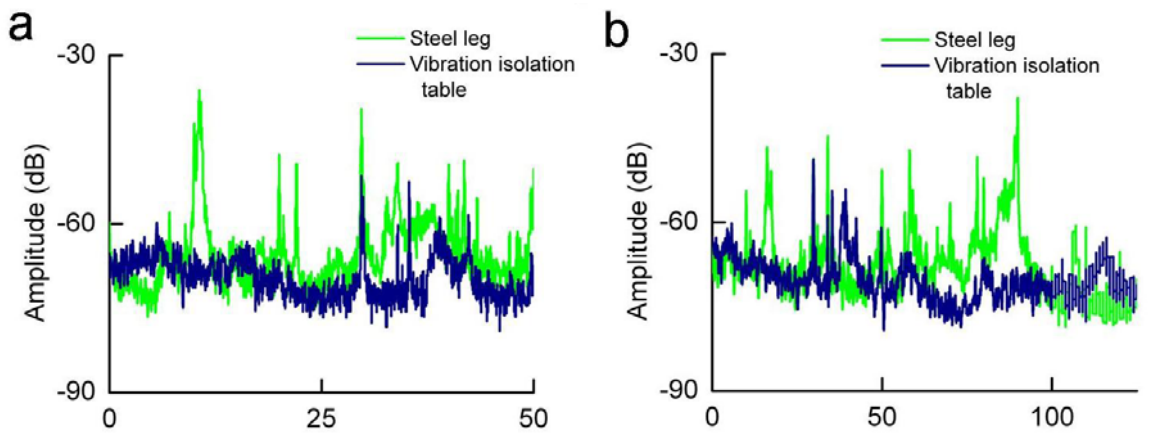

Figure C.4: Vibrational noise characterization for the cryogenic STM/SEM: (a) 0–50Hz vibration levels for the accelerometer attached to the steel leg of the steel support table (no vibration isolation) and for the accelerometer on the bottom aluminum plate of the vibration isolation table (with vibration isolation). (b) 0–125Hz vibration levels for the accelerometer attached to the steel leg of the steel support table (no vibration isolation) and for the accelerometer on the bottom aluminum plate of the vibration isolation table (with vibration isolation).

isolation table.

C.4 Cryogenic operation and STM tip and sample exchange in-situ

Cooling of the STM of the STM/SEM is performed under UHV conditions by a continuous flow cryo-cooler. The cold tip of the cryo-cooler provides the main cooling to the STM head, and the temperature is controlled by adjusting the cryogen flow rate using a fine needle valve on the cold tip and by using a heater wrapped around the cold tip. The cryo-cooler manufacturer also provides a secondary cold connection for an outer thermal radiation shield. The secondary connection point on the cryo-cooler is cooled by helium exhaust gas from the flow of liquid helium internal to the cryo-cooler. Two thermal radiation shields will be used to shield the STM from heat sources. The STM will be linked directly to the cold tip and surrounded by an inner thermal radiation shield connected to the cold tip. An outer thermal radiation shield will be connected to the secondary cold connection and surround the STM and inner radiation shield. Should mechanical vibrations

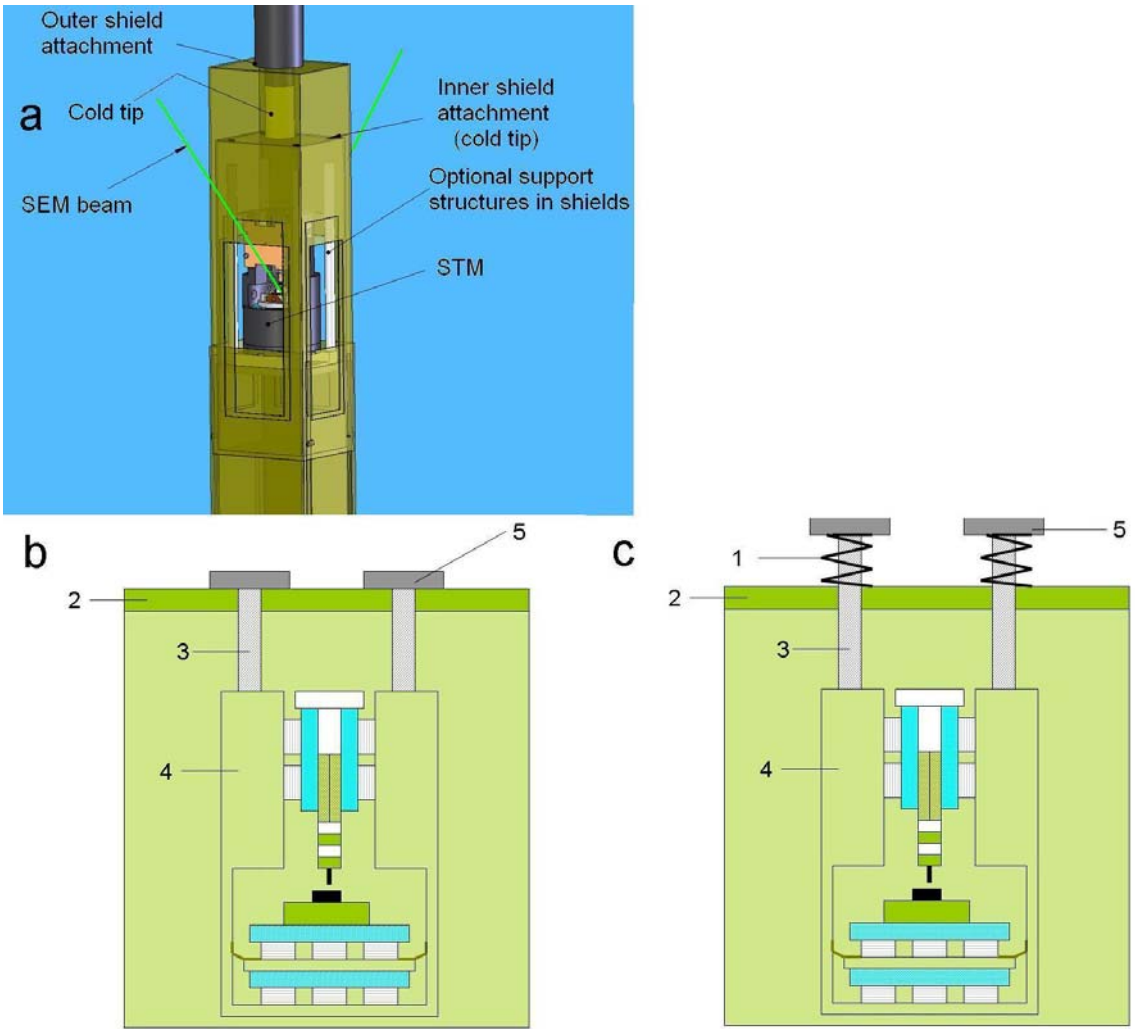

Figure C.5: Illustration of thermal radiation shields for the cryogenic STM/SEM: (a) Two-dimensional image of the solid model for the inner and outer thermal radiation shields of the cryogenic STM/SEM and their attachments to the continuous flow cryo-cooler. The inner radiation shield attaches directly to the cold tip of the cryo-cooler. The outer thermal radiation shield attaches to the secondary cold connection of the cryo-cooler, which is cooled by returning helium gas inside the cryo-cooler. The shields are designed to lower for tip and sample exchange and raise for STM/SEM measurements. Small holes, to allow the SEM beam to reach the STM sample stage and to allow the secondary and backscattered electrons to be detected, will eventually need to be cut into the shields. [1]–Compression springs, [2]–Inner shield attachment: Top plate of the inner radiation shield which attaches directly to the cold tip, [3]–#10-32 Stainless steel (SS) threaded rod. The SS rod is threaded into the STM head. The SS threaded rod fits through a through-hole in the inner shield attachment, and may be secured directly to the inner shield attachment using washers and nuts or compression springs may be added, [4]–STM head inside the inner radiation shield, [5]–Attachment point for design (b) or large washers to hold the compression springs in place for design (c). (b) Current design for attaching the STM head to the inner radiation shield. This design will minimize vibrations between STM and SEM. The STM may not achieve atomic resolution constant-current imaging capability in this design, and it may be necessary to use the secondary design. (c) Secondary design for attaching the STM head to the inner radiation shield and cold tip. Compression springs can be placed between the top of the inner radiation shield and the SS threaded rod to provide local vibration damping to the STM head. The relative vibration between the STM head and the SEM will be increased compared to the current design in the secondary design.

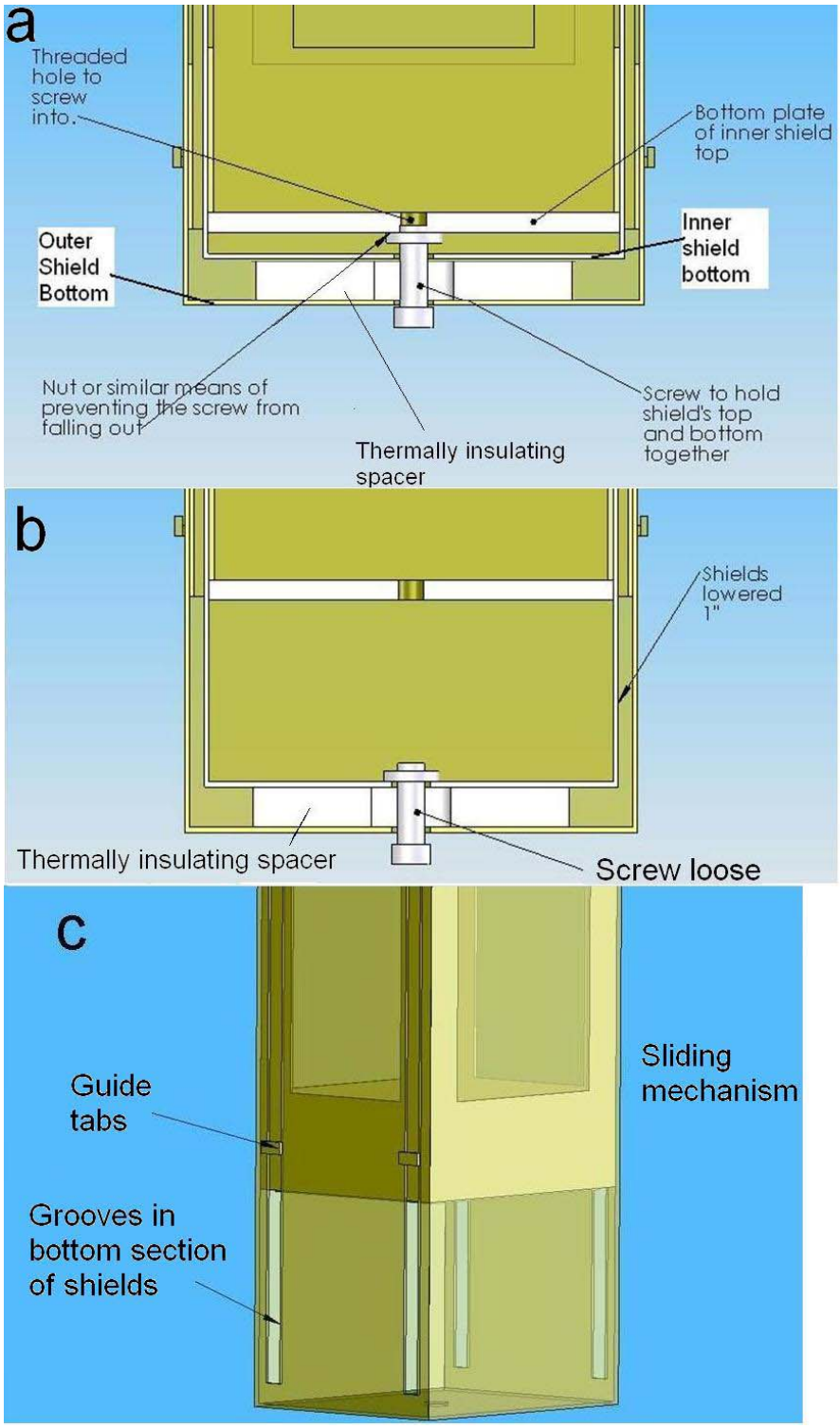

Figure C.6: Illustration of the design of the inner and outer thermal radiation shields: (a) Schematic of the inner and outer thermal radiation shields in the raised position. A screw holds the two shields together in the raised position. (b) Shields lowered by undoing the screw holding them together. The wobble stick ([5] in Fig. C.1) attached to the main analysis chamber of the STM/SEM will be used to manipulate the screw to raise and lower the thermal radiation shields, as shown in Fig. C.7. (c) Illustration of the guiding tabs grooves that comprise the guided sliding mechanism of the thermal radiation shields.

from direct connection of the STM to the cold tip be too large for atomic resolution imaging with the STM, a secondary design, utilizing compression springs between the STM head and the inner thermal radiation shield connection, will reduce mechanical vibrations at the STM head. Both thermal radiation shields and the secondary design for compression spring connections are illustrated in Figs. C.5 and C.6.

In order to exchange samples and tips, the thermal radiation shields must be lowered to provide access to the STM stage. The schematic process for lowering the shields is shown in Fig. C.7. Initially, the radiation shields are in place and raised for STM measurements. The STM and radiation shields are then lowered to the bottom of the main analysis chamber[27] (hidden in Fig. C.7) in order to loosen the set screw holding the thermal shields up. Once the screw has been loosened, the STM is raised up and the thermal radiation shield will lower. Subsequently, the STM may be rotated via the Omniax XYZ and rotary (XYZR) manipulator in order for the tip and sample to be exchanged via the linear, rotary manipulator shown in Fig. C.1. The process is reversed once a tip and sample have been loaded to raise the thermal radiation shields for STM and SEM measurements to be performed in the top portion of the main analysis chamber.

The schematic process of exchanging a tip is shown in Fig. C.8. The linear, rotary manipulator will have a threaded attachment on the end of the manipulator which can be threaded through a removable sample stage ([8] in Fig. C.2). The sample stage may then be interlocked into the fixed OFHC copper stage ([7] in Fig. C.2). The linear, rotary manipulator may then be unscrewed and removed. A special sample stage for holding tips for exchange may also be constructed. A schematic of one design for exchanging tips in this manner is shown in Fig. C.8c,d. A spring loaded tip-grabbing feature on the end of the tube scanner can be used to grab a tip and pull it back for use in such a design.

[27] Control of the Omniax XYZR manipulator is performed through stepper motors and the Sim-Step stepper motor controller purchased from VG Scienta, Inc.

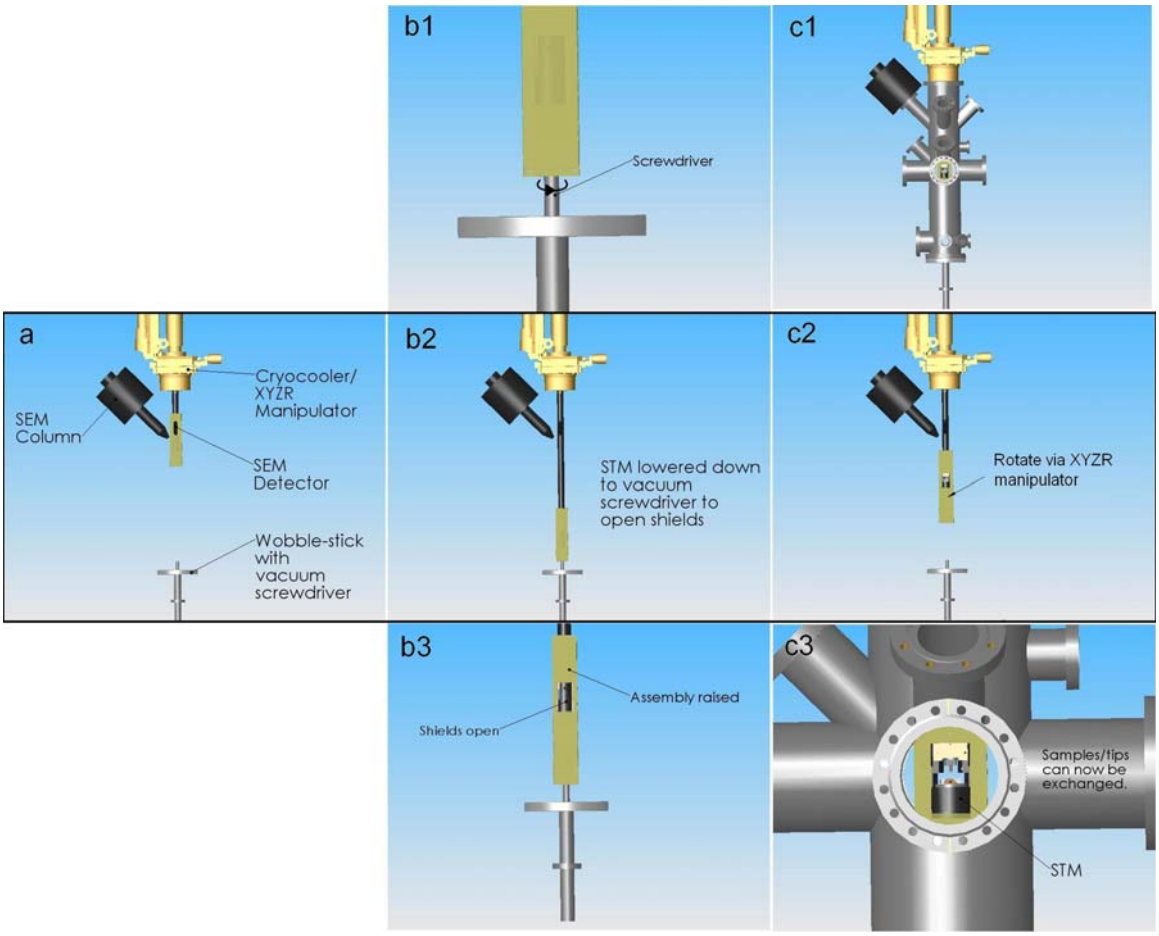

Figure C.7: Schematic illustration of raising and lowering the thermal radiation shields: The images illustrate the parts inside the main analysis chamber. The main analysis chamber is hidden except in (c1) and (c3). (a) The thermal radiation shields are raised and the STM is in the upper portion of the main analysis chamber of the STM/SEM for simultaneous STM and SEM study. (b) The XYZR ([2] in Fig. C.1) manipulator may then be used to lower the radiation shields down to the wobble stick to unscrew the screw shown in Fig. C.6: (b1) Illustrating the wobble stick unscrewing the thermal radiation shield screw. (b2) The thermal radiation shields lowered to the wobble stick using the XYZR manipulator. (b3) After the thermal radiation screw is loose, the entire STM assembly may be raised using the XYZR manipulator, and the shield bottoms will lower due to gravity. (c) The STM assembly may then be rotated and raised to the proper height for tip and sample exchange. (c1) The STM assembly raised to the proper height for tip and sample exchange with the main analysis chamber of the STM/SEM shown. (c2) The STM assembly raised to the proper height for tip and sample exchange without the main analysis chamber of the STM/SEM shown for comparison with (a) and (b). (c3) Zoomed in view of the STM assembly raised to the proper height for tip and sample exchange with the main analysis chamber of the STM/SEM shown. The linear, rotary manipulator can be used to exchange tips and samples. More details are described in Fig. C.8.

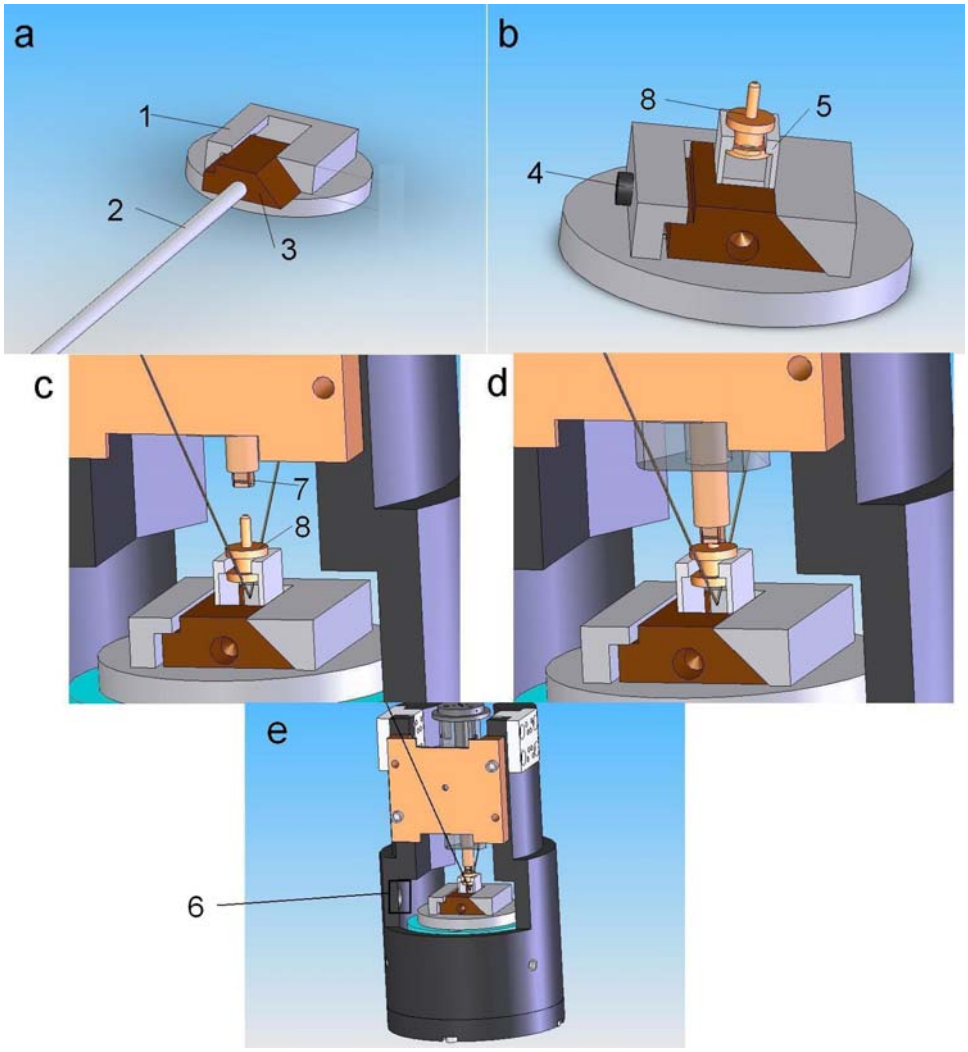

Figure C.8: Schematic of the tip and sample exchange mechanism for the cryogenic STM/SEM: [1]–Schematic of the fixed OFHC sample stage of the STM head ([7] in Fig. C.2)[2]–Linear, rotary manipulator ([10] in Fig. C.1) with a threaded attachment on the end, [3]–Schematic of the removable OFHC sample stage of the STM head ([6] in Fig. C.2). The removable stage has a threaded hole in the center of its face for attachment to the threaded end of the linear, rotary manipulator, [4]–Stainless steel set screw for holding the removable OFHC sample stage in place, [5] Additional attachment for removable OFHC sample stages for tip exchange, [6] Through-hole for the linear rotary manipulator to tighten the set screw to secure the removable sample stage, [7] STM tip grip piece. Initially designed to be a copper-beryllium spring loaded grip piece, [8]–Removable STM tip holder. (a) Schematic illustration of a removable OFHC sample stage ([3]) being inserted into the fixed OFHC sample stage ([1]). Once the removable stage is completely inserted into the fixed stage, the linear, rotary manipulator may be unscrewed from the fixed sample stage. (b) Schematic illustration of an additional attachment for tip exchange and the set screw for securing the sample stage. The STM assembly may be rotated using the XYZR manipulator so that the set screw is accessible through the set screw hole ([6]) in order to secure the removable OFHC sample stages. (c) Schematic illustration of tip exchange. The piezo tube scanner is equipped with an attachment ([7]) that may be used to grab the removable tip holder ([8]). (d) The Z coarse-motion stage may be used to lower the piezo tube scanner to grab the removable tip holder ([8]). (e) Zoomed out view of the STM head for comparison with (c) and (d).